PNC TN9410 98-005

FOR PUBLICATION

Phase Change Predictions for Liquid Fuel in Contact with Steel Structure using the Heat Conduction Equation

January 1998

O-arai Engineering Center

Power Reactor and Nuclear Fuel Development Corporation

Ⓢ

PNC TN9410 98-005
January, 1998

Phase Change Predictions for Liquid Fuel in contact with Steel Structure using the Heat Conduction Equation

David J. Brear *

ABSTRACT

When liquid fuel makes contact with steel structure the liquid can freeze as a crust and the structure can melt at the surface. The melting and freezing processes that occur can influence the mode of fuel freezing and hence fuel relocation. Furthermore the temperature gradients established in the fuel and steel phases determine the rate at which heat is transferred from fuel to steel. In this memo the 1-D transient heat conduction equations are applied to the case of initially liquid UO_2 brought into contact with solid steel using up-to-date materials properties. The solutions predict criteria for fuel crust formation and steel melting and provide a simple algorithm to determine the interface temperature when one or both of the materials is undergoing phase change. The predicted steel melting criterion is compared with available experimental results.

* International Fellow, Fast Reactor Engineering Section, Safety Engineering Division, O-arai Engineering Center, PNC

公　開　資　料
PNC TN9410 98-005
1 9 9 8 年 1 月

熱伝導方程式を用いた
スティール構造材と接触した溶融燃料の相変化予測

David J. Brear *

要旨

仮想的な炉心損傷事故時において、溶融燃料は燃料集合体ラッパ管等のスティール構造材と接触した場合には、燃料は固化して構造材表面にクラストを形成するとともに、構造材の表面は溶融する可能性がある。このような溶融・固化過程は、燃料の固化挙動、すなわち燃料の炉心からの流出挙動に影響を及ぼす。この場合、燃料およびスティールの中に形成される温度勾配によって、燃料からスティールへの熱移行速度が計算されることになる。本研究では、初期に液体状態にあるUO_2が固体スティールに接触する場合に１次元非定常熱伝導方程式を適用し、最新の物性値を用いることで、燃料クラストの形成およびスティール溶融が生じる条件を予測した。また、その一方もしくは両方の物質が相変化する時の界面温度を計算するための簡易解析手法を作成した。本研究で予測されたスティール溶融条件を既存の実験結果と比較して、モデルの妥当性を確認した。

＊ 大洗工学センター、安全工学部、高速炉安全工学室、国際特別研究員

Phase Change Predictions for Liquid Fuel in contact with Steel Structure using the Heat Conduction Equation

TABLE OF CONTENTS

LIST OF TABLES, FIGURES AND APPENDICES

Tables

Figures

Figures continued

Appendices

NOMENCLATURE

Arabic symbols

c	specifc heat of constant volume
D_h	hydraulic diameter
h_l	heat transfer coefficient in the liquid
k	thermal conductivity
L	latent heat
Nu	Nusselt number
Pr	Prandtl number
q	heat flux
Q	relative energy transfer
Re	Reynolds number
t	time
T	temperature
V	velocity
x	location (from the interface separating the two materials)
X	location to phase change fronts from the interface (see Fig. 1)

Greek symbols

α	thermal diffusivity $= k/\rho c$
δ	hydrodynamic boundary layer in the liquid
Δ	thermal lengthscale in the liquid
λ	dimensionless location of phase change front (see eqns 2.7 & 2.15)
ρ	density
μ	viscosity

Subscripts

1	material 1
2	material 2
fu	fuel (UO_2)
i	interface
l	liquid
L	latent heat
mp	melting point
s	solid
ss	stainless steel

NOMENCLATURE (continued)

Variables groupings

Temperature differences (see Figure 2):

$\Delta T_{mp} = T_{1,mp} - T_{2,mp}$

$\Delta T_1 = T_{1,\infty} - T_{1,mp}$

$\Delta T_2 = T_{2,mp} - T_{2,\infty}$

Dimensionless groupings:

$$\beta_1 = \left(\frac{\alpha_{1,s}}{\alpha_{1,l}}\right)^{1/2} \qquad \beta_2 = \left(\frac{\alpha_{2,l}}{\alpha_{2,s}}\right)^{1/2}$$

$$\omega_{1,l} = (\rho ck)_{1,l}^{1/2} \qquad \omega_{1,s} = (\rho ck)_{1,s}^{1/2} \qquad \omega_{2,l} = (\rho ck)_{2,l}^{1/2} \qquad \omega_{2,s} = (\rho ck)_{2,s}^{1/2}$$

$$\Lambda_1 = \frac{\pi^{1/2} L_1}{c_{1,s}\Delta T_{mp}} \qquad \Lambda_2 = \frac{\pi^{1/2} L_2}{c_{2,l}\Delta T_{mp}}$$

1. INTRODUCTION

When liquid fuel makes contact with steel structure the fuel can freeze to form a stable crust, or can melt and ablate the structure. The type of phase change which occurs can be important for predicting events during a hypothetical Core Disruptive Accident (CDA). To assess the freezing behaviour of liquid fuel on steel structures it is necessary to establish whether fuel freezes or steel melts when they come into contact.

On very short timescales the heat transfer in the fuel and steel is dominated by transient heat conduction. One way to determine the type of phase change is to solve the transient heat conduction equations for the case of initially liquid UO_2 in perfect thermal contact with solid steel. This type of analysis was originally performed by Epstein [1] and key results are shown in Figure 1. The results of Epstein's analysis are still widely used to predict the temperature conditions under which steel structure is melted and ablated.

The results published in ref. [1] are not very detailed and were obtained with old values of materials properties, many of which have since been updated. Furthermore the calculations reported in ref. [2] indicate that it is necessary to take account of the temperature-dependence of steel properties if reasonably accurate results are to be obtained. Moreover all published results are specific to the UO_2-steel system, and it is desirable to extend the analysis to other combinations of materials which are used in out-of-pile freezing tests.

This memo repeats and extends the heat conduction analysis. The solutions of the heat conduction equation for selected pairs of UO_2 and steel initial temperatures are evaluated using a small computer code. The use of a computer code makes it convenient to perform recalculations to investigate the effect of uncertainties, to replace materials properties, and to evaluate the influence of temperature-variation in materials properties. The up-to-date materials properties in the SIMMER-III computer code [3] have been used to perform the calculations. Furthermore two approximate formulations are described and compared to the exact transient solutions. Finally the effect of an idealized gap conductance is described.

This report is structured as follows. The analytical solutions to the transient conduction equations for a hot liquid in perfect thermal contact with a relatively cold solid are written down in Section 2. Approximate, but simpler, solutions to the transient conduction equations are derived in Section 3, and the effect of imperfect thermal contact is discussed in Section 4. Finally interface temperatures and fuel freezing/steel melting criteria for liquid UO_2 making contact with steel structure are described in Section 5. The steel melting criterion is compared with experimental data in Section 5.5.

2. FORMULATION OF THE EXACT SOLUTION FOR PERFECT CONTACT

2.1 Geometry and assumptions

A hot liquid (material 1) is suddenly brought into contact with cold, solid structure (material 2). The melting temperature of the hot liquid is higher than the melting point of the structure. At the contact surface (the interface) the liquid may solidify and/or the structure may melt, as illustrated in Figure 2. The phase change is determined by the transient temperature response of the two materials. If the liquid freezes it is assumed to form a crust on the surface; if the structure melts it is assumed to form a stationary liquid layer. Other assumptions are:

- The geometry is 1-D: a semi-infinite body of liquid at uniform temperature suddenly makes contact with a semi-infinite structure at uniform temperature.
- The only heat transfer mechanism is thermal conduction (liquid convection is neglected). Crust growth is controlled by heat conduction only.
- The phase transitions - liquid freezing and structure melting - take place at a single temperature. The latent heat of fusion is liberated (or absorbed) at the equilibrium melting temperature. (A single melting temperature can be assumed for pure UO_2, but steel melts between a solidus temperature of 1713 K and a liquidus temperature of 1753 K.)
- The volume change associated with solidification or melting can be ignored.
- There is perfect thermal contact between liquid and structure, and a gap does not form between a crust and structure.
- The four phases that can be present have constant materials properties.

The temperature profile in both materials is dictated by the transient heat conduction equation. Assuming constant materials properties for each phase, the heat conduction equation in one-dimension is:

$$\frac{\partial T(x,t)}{\partial t} = \alpha \frac{\partial T(x,t)}{\partial x^2} \tag{2.1}$$

A general solution of equation (2.1) is:

$$T(x,t) = A + B \times \mathrm{erf}\left(\frac{x}{2(\alpha t)^{1/2}}\right) \tag{2.2}$$

where A and B are constants, and the error function erf(z) is described in Appendix A. (Nomenclature and variables are defined at the front of this memo, and are illustrated in Figure 2.)

The time-dependent temperature profiles obtained from equation (2.1) are described in the Sections 2.2 to 2.5 for the four possible phase change combinations: (a) neither material undergoes a phase change, (b) the liquid freezes to form a crust but the structure does not melt, (c) the liquid does not

freeze, but the structure melts at the surface, and (d) the liquid freezes and the structure melts simultaneously. The latter scenario is illustrated in Figure 2.

The phase change criteria, which determine the temperature conditions for which the liquid freezes and the structure melts, are described in Section 2.6. Although the solutions of equation (2.1) are temperature profiles, time-invariant quantities are the most important results: the temperature at the interface, the solidification and melting constants, and the proportion of heat transferred to or from the various phases.

2.2 Solution when neither material undergoes a phase change

Only the liquid of material 1 and the solid of material 2 are considered. Temperatures and heat fluxes are continuous at the interface.

Boundary conditions

$$\begin{aligned} &T_{1,l} \to T_{1,\infty} \quad \text{as} \quad x \to -\infty \\ &T_{1,l} = T_{2,s} = T_i \quad \text{at} \quad x = 0 \\ &T_{2,s} \to T_{2,\infty} \quad \text{as} \quad x \to \infty \\ &-k_{1,l}\left.\frac{\partial T_{1,l}}{\partial x}\right|_{x=0} = -k_{2,s}\left.\frac{\partial T_{2,s}}{\partial x}\right|_{x=0} \end{aligned} \tag{2.3}$$

Solution

$$\begin{aligned} T_{1,l} &= T_i - \left(T_{1,\infty} - T_i\right)\mathrm{erf}\left(\frac{x}{2\left(\alpha_{1,l}t\right)^{1/2}}\right) \\ T_{2,s} &= T_i - \left(T_i - T_{2,\infty}\right)\mathrm{erf}\left(\frac{x}{2\left(\alpha_{2,s}t\right)^{1/2}}\right) \end{aligned} \tag{2.4}$$

where the interface temperature is given by:

$$T_i = \frac{\omega_{1,l}T_{1,\infty} + \omega_{2,s}T_{2,\infty}}{\left(\omega_{1,l} + \omega_{2,s}\right)} \tag{2.5}$$

Equation (2.5) is the formula used to define the interface temperature for a number of heat and mass transfer paths in SIMMER-III. Strictly speaking, equation (2.5) is applicable only if the interface temperature T_i is above the melting point of material 1 and below the melting point of material 2.

2.3 Solution when liquid material 1 freezes, solid material 2 does not melt

A crust, solid material 1, is formed at the interface, and a solidification front advances into the liquid. The liquid-crust interface temperature is the equilibrium melting point of material 1.

Boundary conditions

$$
\begin{aligned}
&T_{1,l} \to T_{1,\infty} \qquad \text{as} \qquad x \to -\infty \\
&T_{1,l} = T_{1,s} = T_{1,mp} \qquad \text{at} \qquad x = X_1(t) \\
&T_{1,s} = T_{2,s} = T_i \qquad \text{at} \qquad x = 0 \\
&T_{2,s} \to T_{2,\infty} \qquad \text{as} \qquad x \to \infty \\
&-k_{1,l}\left.\frac{\partial T_{1,l}}{\partial x}\right|_{x=X_1} + k_{1,s}\left.\frac{\partial T_{1,s}}{\partial x}\right|_{x=X_1} = L_1\rho_1\frac{dX_1}{dt} \qquad (2.6) \\
&-k_{1,s}\left.\frac{\partial T_{1,s}}{\partial x}\right|_{x=0} = -k_{2,s}\left.\frac{\partial T_{2,s}}{\partial x}\right|_{x=0}
\end{aligned}
$$

Solution

The phase change front is defined in terms of a dimensionless constant, λ_1, which controls the rate at which the freezing front penetrates liquid 1:

$$X_1(t) = -2\lambda_1\left(\alpha_{1,s}t\right)^{1/2} \qquad (2.7)$$

The temperature profiles are then:

$$
\begin{aligned}
T_{1,l} &= T_{1,\infty} - \frac{\Delta T_1}{\left(1-\operatorname{erf}\left(\beta_1\lambda_1\right)\right)}\left(1+\operatorname{erf}\left(\frac{x}{2\left(\alpha_{1,l}t\right)^{1/2}}\right)\right) \\
T_{1,s} &= T_i - \frac{\left(T_{1,mp}-T_i\right)}{\operatorname{erf}\left(\lambda_1\right)}\operatorname{erf}\left(\frac{x}{2\left(\alpha_{1,s}t\right)^{1/2}}\right) \qquad (2.8) \\
T_{2,s} &= T_i - \left(T_i - T_{2,\infty}\right)\operatorname{erf}\left(\frac{x}{2\left(\alpha_{2,s}t\right)^{1/2}}\right)
\end{aligned}
$$

where the interface temperature is given by:

$$T_i = \frac{\left(\omega_{1,s}/\operatorname{erf}\left(\lambda_1\right)\right)T_{1,mp} + \omega_{2,s}T_{2,\infty}}{\left(\left(\omega_{1,s}/\operatorname{erf}\left(\lambda_1\right)\right) + \omega_{2,s}\right)} \qquad (2.9)$$

The interface temperature of equation (2.9) is below the melting temperature of material 2 and above its initial temperature. λ_1 is obtained by solving the following transcendental equation:

$$\frac{\omega_{2,s}e^{-\lambda_1^2}}{\left(\omega_{1,s}+\omega_{2,s}\mathrm{erf}(\lambda_1)\right)}\left(1+\frac{\Delta T_2}{\Delta T_{mp}}\right)-\frac{e^{-\beta_1^2\lambda_1^2}}{\mathrm{erfc}(\beta_1\lambda_1)}\frac{\omega_{1,l}}{\omega_{1,s}}\frac{\Delta T_1}{\Delta T_{mp}}=\Lambda_1\lambda_1 \qquad (2.10)$$

Equation (2.10) is actually the energy conservation equation for the system. The total heat flux from material 1 to material 2, the heat flux from liquid material 1 to solid material 1, the rate of latent heat liberated by the freezing of material 1, and the net heat flux out of solid material 1 are given respectively by:

$$\begin{aligned}
q_{1,t} &= -k_{1,s}\left.\frac{\partial T_{1,s}}{\partial x}\right|_{x=0} = \frac{\omega_{1,s}\omega_{2,s}}{\left(\omega_{1,s}+\omega_{2,s}\mathrm{erf}(\lambda_1)\right)}\cdot\frac{\left(\Delta T_{mp}+\Delta T_2\right)}{\sqrt{\pi t}}\\
q_{1,l} &= -k_{1,l}\left.\frac{\partial T_{1,l}}{\partial x}\right|_{x=X_1} = \frac{e^{-\beta_1^2\lambda_1^2}}{\mathrm{erfc}(\beta_1\lambda_1)}\cdot\frac{\omega_{1,l}\Delta T_1}{\sqrt{\pi t}}\\
q_{1,L} &= -L_1\rho_1\frac{dX_1}{dt} = \Lambda_1\lambda_1\cdot\frac{\omega_{1,s}\Delta T_{mp}}{\sqrt{\pi t}} \qquad (2.11)\\
q_{1,s} &= +k_{1,s}\left.\frac{\partial T_{1,s}}{\partial x}\right|_{x=X_1} - k_{1,s}\left.\frac{\partial T_{1,s}}{\partial x}\right|_{x=0} = \frac{\omega_{1,s}\omega_{2,s}\left(1-e^{-\lambda_1^2}\right)}{\left(\omega_{1,s}+\omega_{2,s}\mathrm{erf}(\lambda_1)\right)}\cdot\frac{\left(\Delta T_{mp}+\Delta T_2\right)}{\sqrt{\pi t}}
\end{aligned}$$

The proportion of the total heat lost at all times from material 1 - from the liquid, from the liberated latent heat and from the solid respectively - can be obtained from equation (2.11) by dividing the latter three equalities by the first equality:

$$\begin{aligned}
Q_{1,l} &= \frac{e^{-\beta_1^2\lambda_1^2}}{\mathrm{erfc}(\beta_1\lambda_1)}\cdot\omega_{1,l}\cdot\left(\mathrm{erf}(\lambda_1)/\omega_{1,s}+1/\omega_{2,s}\right)\cdot\frac{\Delta T_1}{\left(\Delta T_{mp}+\Delta T_2\right)}\\
Q_{1,L} &= \Lambda_1\lambda_1\cdot\left(\mathrm{erf}(\lambda_1)+\omega_{1,s}/\omega_{2,s}\right)\cdot\frac{1}{\left(1+\Delta T_2/\Delta T_{mp}\right)} \qquad (2.12)\\
Q_{1,s} &= \left(1-e^{-\lambda_1^2}\right)
\end{aligned}$$

Equation (2.10) is therefore compatible with energy conservation:

$$Q_{1,l}+Q_{1,L}+Q_{1,s}=1 \qquad (2.13)$$

2.4 Solution when solid material 2 melts, liquid material 1 does not freeze

The structure, material 2, melts at the interface, and a melting front advances into material 2. The temperature at the melting front is the equilibrium temperature of material 2.

Boundary conditions

$$
\begin{aligned}
&T_{1,l} \rightarrow T_{1,\infty} \quad \text{as} \quad x \rightarrow -\infty \\
&T_{1,l} = T_{2,l} = T_i \quad \text{at} \quad x = 0 \\
&T_{2,l} = T_{2,s} = T_{2,mp} \quad \text{at} \quad x = X_2(t) \\
&T_{2,s} \rightarrow T_{2,\infty} \quad \text{as} \quad x \rightarrow \infty \\
&-k_{1,l}\left.\frac{\partial T_{1,l}}{\partial x}\right|_{x=0} = -k_{2,l}\left.\frac{\partial T_{2,l}}{\partial x}\right|_{x=0} \\
&-k_{2,l}\left.\frac{\partial T_{2,l}}{\partial x}\right|_{x=X_2} + k_{2,s}\left.\frac{\partial T_{2,s}}{\partial x}\right|_{x=X_2} = L_2\rho_2\frac{dX_2}{dt}
\end{aligned}
\tag{2.14}
$$

Solution

The phase change front is defined in terms of a dimensionless constant, λ_2, which controls the rate at which the melting front penetrates material 2:

$$X_2(t) = 2\lambda_2\left(\alpha_{2,l}t\right)^{1/2} \tag{2.15}$$

The temperature profiles are then:

$$
\begin{aligned}
T_{1,l} &= T_i - \left(T_{1,\infty} - T_i\right)\operatorname{erf}\left(\frac{x}{2\left(\alpha_{1,l}t\right)^{1/2}}\right) \\
T_{2,l} &= T_i - \frac{\left(T_i - T_{2,mp}\right)}{\operatorname{erf}(\lambda_2)}\operatorname{erf}\left(\frac{x}{2\left(\alpha_{2,l}t\right)^{1/2}}\right) \\
T_{2,s} &= T_{2,\infty} + \frac{\Delta T_2}{\left(1-\operatorname{erf}(\beta_2\lambda_2)\right)}\left(1-\operatorname{erf}\left(\frac{x}{2\left(\alpha_{2,s}t\right)^{1/2}}\right)\right)
\end{aligned}
\tag{2.16}
$$

where the interface temperature is given by:

$$T_i = \frac{\omega_{1,l}T_{1,\infty} + \left(\omega_{2,l}/\operatorname{erf}(\lambda_2)\right)T_{2,mp}}{\left(\omega_{1,l} + \left(\omega_{2,l}/\operatorname{erf}(\lambda_2)\right)\right)} \tag{2.17}$$

The interface temperature of equation (2.17) is above the melting temperature of liquid 1 and above the initial temperature of material 1. λ_2 is obtained by solving the following transcendental equation:

$$\frac{\omega_{1,l}e^{-\lambda_2^2}}{\left(\omega_{2,l}+\omega_{1,l}\mathrm{erf}(\lambda_2)\right)}\left(1+\frac{\Delta T_1}{\Delta T_{mp}}\right)-\frac{e^{-\beta_2^2\lambda_2^2}}{\mathrm{erfc}(\beta_2\lambda_2)}\frac{\omega_{2,s}}{\omega_{2,l}}\frac{\Delta T_2}{\Delta T_{mp}}=\Lambda_2\lambda_2 \tag{2.18}$$

Equation (2.18) is actually the energy conservation equation for the system. The total heat flux from material 1 to material 2, the net heat flux into liquid material 2, the rate of latent heat absorbed by the melting of material 2, and the net heat flux into solid material 2 are given respectively by:

$$\begin{aligned}
q_{2,t} &= -k_{2,l}\left.\frac{\partial T_{2,l}}{\partial x}\right|_{x=0} = \frac{\omega_{1,l}\omega_{2,l}}{\left(\omega_{1,l}\mathrm{erf}(\lambda_2)+\omega_{2,l}\right)}\cdot\frac{\left(\Delta T_{mp}+\Delta T_1\right)}{\sqrt{\pi t}}\\
q_{2,l} &= -k_{2,l}\left.\frac{\partial T_{2,l}}{\partial x}\right|_{x=0} + k_{2,l}\left.\frac{\partial T_{2,l}}{\partial x}\right|_{x=X_2} = \frac{\omega_{1,l}\omega_{2,l}\left(1-e^{-\lambda_2^2}\right)}{\left(\omega_{1,l}\mathrm{erf}(\lambda_2)+\omega_{2,l}\right)}\cdot\frac{\left(\Delta T_{mp}+\Delta T_1\right)}{\sqrt{\pi t}}\\
q_{2,L} &= L_2\rho_2\frac{dX_2}{dt} = \Lambda_2\lambda_2\cdot\frac{\omega_{2,l}\Delta T_{mp}}{\sqrt{\pi t}}\\
q_{2,s} &= -k_{2,s}\left.\frac{\partial T_{2,s}}{\partial x}\right|_{x=X_2} = \frac{e^{-\beta_2^2\lambda_2^2}}{\mathrm{erfc}(\beta_2\lambda_2)}\cdot\frac{\omega_{2,s}\Delta T_2}{\sqrt{\pi t}}
\end{aligned} \tag{2.19}$$

The proportion of the total heat gained at all times by material 2 - by the liquid, by the absorbed latent heat and by the solid respectively - can be obtained from equation (2.19) by dividing the latter three equalities by the first equality:

$$\begin{aligned}
Q_{2,l} &= \left(1-e^{-\lambda_2^2}\right)\\
Q_{2,L} &= \Lambda_2\lambda_2\cdot\left(\mathrm{erf}(\lambda_2)+{}^{\omega_{2,l}}\!/_{\omega_{1,l}}\right)\cdot\frac{1}{\left(1+{}^{\Delta T_1}\!/_{\Delta T_{mp}}\right)}\\
Q_{2,s} &= \frac{e^{-\beta_2^2\lambda_2^2}}{\mathrm{erfc}(\beta_2\lambda_2)}\cdot\omega_{2,s}\cdot\left({}^{\mathrm{erf}(\lambda_2)}\!/_{\omega_{2,l}}+{}^{1}\!/_{\omega_{1,l}}\right)\cdot\frac{\Delta T_2}{\left(\Delta T_{mp}+\Delta T_1\right)}
\end{aligned} \tag{2.20}$$

Equation (2.18) is therefore compatible with energy conservation:

$$Q_{2,l}+Q_{2,L}+Q_{2,s}=1 \tag{2.21}$$

2.5 Solution when there is simultaneous melting and freezing at the interface

The liquid freezes and the solid structure melts at the interface, as shown in Figure 1. A solidification front moves into material 1 and at the same time a melting front moves into material 2.

Boundary conditions

$$
\begin{aligned}
&T_{1,l} \to T_{1,\infty} \quad \text{as} \quad x \to -\infty \\
&T_{1,l} = T_{1,s} = T_{1,mp} \quad \text{at} \quad x = X_1(t) \\
&T_{1,s} = T_{2,l} = T_i \quad \text{at} \quad x = 0 \\
&T_{2,l} = T_{2,s} = T_{2,mp} \quad \text{at} \quad x = X_2(t) \\
&T_{2,s} \to T_{2,\infty} \quad \text{as} \quad x \to \infty \\
&-k_{1,l}\left.\frac{\partial T_{1,l}}{\partial x}\right|_{x=X_1} + k_{1,s}\left.\frac{\partial T_{1,s}}{\partial x}\right|_{x=X_1} = L_1\rho_1\frac{dX_1}{dt} \\
&-k_{1,s}\left.\frac{\partial T_{1,s}}{\partial x}\right|_{x=0} = -k_{2,l}\left.\frac{\partial T_{2,l}}{\partial x}\right|_{x=0} \\
&-k_{2,l}\left.\frac{\partial T_{2,l}}{\partial x}\right|_{x=X_2} + k_{2,s}\left.\frac{\partial T_{2,s}}{\partial x}\right|_{x=X_2} = L_2\rho_2\frac{dX_2}{dt}
\end{aligned}
\tag{2.22}
$$

Solution

Let the phase change fronts be rewritten in terms of the dimensionless constants defined in equations (2.7) and (2.15). The temperature profiles are then:

$$
\begin{aligned}
T_{1,l} &= T_{1,\infty} - \frac{\Delta T_1}{\left(1-\operatorname{erf}(\beta_1\lambda_1)\right)}\left(1+\operatorname{erf}\left(\frac{x}{2(\alpha_{1,l}t)^{1/2}}\right)\right) \\
T_{1,s} &= T_i - \frac{\left(T_{1,mp}-T_i\right)}{\operatorname{erf}(\lambda_1)}\operatorname{erf}\left(\frac{x}{2(\alpha_{1,s}t)^{1/2}}\right) \\
T_{2,l} &= T_i - \frac{\left(T_i-T_{2,mp}\right)}{\operatorname{erf}(\lambda_2)}\operatorname{erf}\left(\frac{x}{2(\alpha_{2,l}t)^{1/2}}\right) \\
T_{2,s} &= T_{2,\infty} + \frac{\Delta T_2}{\left(1-\operatorname{erf}(\beta_2\lambda_2)\right)}\left(1-\operatorname{erf}\left(\frac{x}{2(\alpha_{2,s}t)^{1/2}}\right)\right)
\end{aligned}
\tag{2.23}
$$

where the interface temperature is given by:

$$T_i = \frac{\left(\omega_{1,s}/\mathrm{erf}(\lambda_1)\right)T_{1,mp} + \left(\omega_{2,l}/\mathrm{erf}(\lambda_2)\right)T_{2,mp}}{\left(\left(\omega_{1,s}/\mathrm{erf}(\lambda_1)\right) + \left(\omega_{2,l}/\mathrm{erf}(\lambda_2)\right)\right)} \tag{2.24}$$

The interface temperature of equation (2.24) lies below the melting temperature of liquid 1 and above the melting temperature of liquid 2. The solidification and melting constants are obtained from the following transcendental equations:

$$\begin{aligned}
&\frac{\omega_{2,l}e^{-\lambda_1^2}}{\left(\omega_{1,s}\mathrm{erf}(\lambda_2)+\omega_{2,l}\mathrm{erf}(\lambda_1)\right)} - \frac{e^{-\beta_1^2\lambda_1^2}}{\mathrm{erfc}(\beta_1\lambda_1)}\frac{\omega_{1,l}}{\omega_{1,s}}\frac{\Delta T_1}{\Delta T_{mp}} = \Lambda_1\lambda_1 \\
&\frac{\omega_{1,s}e^{-\lambda_2^2}}{\left(\omega_{2,l}\mathrm{erf}(\lambda_1)+\omega_{1,s}\mathrm{erf}(\lambda_2)\right)} - \frac{e^{-\beta_2^2\lambda_2^2}}{\mathrm{erfc}(\beta_2\lambda_2)}\frac{\omega_{2,s}}{\omega_{2,l}}\frac{\Delta T_2}{\Delta T_{mp}} = \Lambda_2\lambda_2
\end{aligned} \tag{2.25}$$

Equation (2.25) is actually the energy conservation equation for the system. The heat fluxes previously defined in Sections 2.3 and 2.4 are given in this case by:

$$\begin{aligned}
q_{1,t} &= -k_{1,s}\left.\frac{\partial T_{1,s}}{\partial x}\right|_{x=0} = \frac{\omega_{1,s}\omega_{2,l}}{\left(\omega_{1,s}\mathrm{erf}(\lambda_2)+\omega_{2,l}\mathrm{erf}(\lambda_1)\right)}\cdot\frac{\Delta T_{mp}}{\sqrt{\pi t}} \\
q_{1,l} &= -k_{1,l}\left.\frac{\partial T_{1,l}}{\partial x}\right|_{x=X_l} = \frac{e^{-\beta_1^2\lambda_1^2}}{\mathrm{erfc}(\beta_1\lambda_1)}\cdot\frac{\omega_{1,l}\Delta T_1}{\sqrt{\pi t}} \\
q_{1,L} &= -L_1\rho_1\frac{dX_1}{dt} = \Lambda_1\lambda_1\cdot\frac{\omega_{1,s}\Delta T_{mp}}{\sqrt{\pi t}} \\
q_{1,s} &= -k_{1,s}\left.\frac{\partial T_{1,s}}{\partial x}\right|_{x=X_l} + k_{1,s}\left.\frac{\partial T_{1,s}}{\partial x}\right|_{x=0} = \frac{\omega_{1,s}\omega_{2,l}\left(1-e^{-\lambda_1^2}\right)}{\left(\omega_{1,s}\mathrm{erf}(\lambda_2)+\omega_{2,l}\mathrm{erf}(\lambda_1)\right)}\cdot\frac{\Delta T_{mp}}{\sqrt{\pi t}}
\end{aligned} \tag{2.26}$$

$$\begin{aligned}
q_{2,t} &= -k_{2,l}\left.\frac{\partial T_{2,l}}{\partial x}\right|_{x=0} = \frac{\omega_{1,s}\omega_{2,l}}{\left(\omega_{1,s}\mathrm{erf}(\lambda_2)+\omega_{2,l}\mathrm{erf}(\lambda_1)\right)}\cdot\frac{\Delta T_{mp}}{\sqrt{\pi t}} \\
q_{2,l} &= -k_{2,l}\left.\frac{\partial T_{2,l}}{\partial x}\right|_{x=0} + k_{2,l}\left.\frac{\partial T_{2,l}}{\partial x}\right|_{x=X_2} = \frac{\omega_{1,s}\omega_{2,l}\left(1-e^{-\lambda_2^2}\right)}{\left(\omega_{1,s}\mathrm{erf}(\lambda_2)+\omega_{2,l}\mathrm{erf}(\lambda_1)\right)}\cdot\frac{\Delta T_{mp}}{\sqrt{\pi t}} \\
q_{2,L} &= L_2\rho_2\frac{dX_2}{dt} = \Lambda_2\lambda_2\cdot\frac{\omega_{2,l}\Delta T_{mp}}{\sqrt{\pi t}} \\
q_{2,s} &= -k_{2,s}\left.\frac{\partial T_{2,s}}{\partial x}\right|_{x=X_2} = \frac{e^{-\beta_2^2\lambda_2^2}}{\mathrm{erfc}(\beta_2\lambda_2)}\cdot\frac{\omega_{2,s}\Delta T_2}{\sqrt{\pi t}}
\end{aligned} \tag{2.27}$$

The heat losses and gains as a proportion of the total heat transferred from material 1 to material 2 are:

$$Q_{1,l} = \frac{e^{-\beta_1^2\lambda_1^2}}{\mathrm{erfc}(\beta_1\lambda_1)} \cdot \omega_{1,l} \cdot \left(\mathrm{erf}(\lambda_1)/\omega_{1,s} + \mathrm{erf}(\lambda_2)/\omega_{2,l} \right) \cdot \frac{\Delta T_1}{\Delta T_{mp}}$$

$$Q_{1,L} = \Lambda_1\lambda_1 \cdot \left(\mathrm{erf}(\lambda_1) + \frac{\omega_{1,s}}{\omega_{2,l}} \mathrm{erf}(\lambda_2) \right) \qquad (2.28)$$

$$Q_{1,s} = \left(1 - e^{-\lambda_1^2}\right)$$

$$Q_{2,l} = \left(1 - e^{-\lambda_2^2}\right)$$

$$Q_{2,L} = \Lambda_2\lambda_2 \cdot \left(\mathrm{erf}(\lambda_2) + \frac{\omega_{2,l}}{\omega_{1,s}} \mathrm{erf}(\lambda_1) \right) \qquad (2.29)$$

$$Q_{2,s} = \frac{e^{-\beta_2^2\lambda_2^2}}{\mathrm{erfc}(\beta_2\lambda_2)} \cdot \omega_{2,s} \cdot \left(\mathrm{erf}(\lambda_2)/\omega_{2,l} + \mathrm{erf}(\lambda_1)/\omega_{1,s} \right) \cdot \frac{\Delta T_2}{\Delta T_{mp}}$$

Equation (2.25) is therefore compatible with energy conservation:

$$Q_{1,l} + Q_{1,L} + Q_{1,s} = Q_{2,l} + Q_{2,L} + Q_{2,s} = 1 \qquad (2.30)$$

The relative thickness of the molten material 2 layer divided by the thickness of the frozen material 1 layer is also time-invariant:

$$\left|\frac{X_2}{X_1}\right| = \left(\frac{\alpha_{2,l}}{\alpha_{1,s}}\right)^{1/2} \frac{\lambda_2}{\lambda_1} \qquad (2.31)$$

2.6 The phase change criteria

The two criteria for freezing of liquid material 1 and melting of the solid material 2 at the interface are derived below.

Condition for liquid freezing

This criterion can be obtained by two methods: (a) set the interface temperature to the liquid 1 melting temperature in equation (2.17) and substitute the relationship into equation (2.18), or (b) set $\lambda_1 = 0$ in equation (2.25) (i.e. the solidification front does not advance into the liquid). Both methods give the same criterion:

$$\frac{\Delta T_1}{\Delta T_{mp}} = \frac{\omega_{2,l}}{\omega_{1,l}\mathrm{erf}(\lambda_2)}$$

$$\frac{e^{-\lambda_2^2}}{\mathrm{erf}(\lambda_2)} - \frac{e^{-\beta_2^2\lambda_2^2}}{\mathrm{erfc}(\beta_2\lambda_2)} \frac{\omega_{2,s}}{\omega_{2,l}} \frac{\Delta T_2}{\Delta T_{mp}} = \Lambda_2\lambda_2 \qquad (2.32)$$

Condition for solid melting

This criterion can be obtained by two methods: (a) set the interface temperature to the liquid 2 melting temperature in equation (2.9) and substitute the relationship into equation (2.10), or (b) set $\lambda_2 = 0$ in equation (2.25) (i.e. the melting front does not advance into the solid). Both methods give the same criterion:

$$\frac{\Delta T_2}{\Delta T_{mp}} = \frac{\omega_{1,s}}{\omega_{2,s}\mathrm{erf}(\lambda_1)}$$
$$\frac{e^{-\lambda_1^2}}{\mathrm{erf}(\lambda_1)} - \frac{e^{-\beta_1^2\lambda_1^2}}{\mathrm{erfc}(\beta_1\lambda_1)}\frac{\omega_{1,l}}{\omega_{1,s}}\frac{\Delta T_1}{\Delta T_{mp}} = \Lambda_1\lambda_1 \qquad (2.33)$$

2.7 Comments on solving the equations

The most useful solutions are the time-invariant quantities: the temperature at the interface, the solidification and melting constants, and the proportion of heat transferred to or from the phases.

If there is no phase change for either material, it is straightforward to solve for the interface temperature equation (2.5). Otherwise solutions must be obtained by the following procedure:

- Solve equations (2.32) and (2.33) to determine what phase changes occur for the given pair of initial temperatures in liquid and structure.
- Solve for the solidification and melting constants λ_1 and λ_2 (equation (2.10) or (2.18) or (2.25)).
- Calculate the interface temperatures and the relative heat transfer quantities as appropriate.

Since the solidification and melting constants λ_1 and λ_2 must be solved by an iterative procedure, it is convenient if the solution procedure is written as a computer code. Such a code, and solutions for the liquid UO_2-steel structure system, is described in Section 5.

3. APPROXIMATE SOLUTIONS FOR PERFECT THERMAL CONTACT

Exact solutions to the transient heat conduction equations described in Section 2 contain the error function as well as the solidification and melting constants λ_1 and λ_2. These variables are complicated to evaluate, especially since λ_1 and λ_2 must be obtained by iteration to solve a pair of transcendental equations. This section describes two approaches which simplify the calculations by using approximate solutions:

- The Amateur Mathematician approach (Section 3.1) attempts to simplify the exact equations by replacing the error function with a polynomial function.
- The Naive Physicist approach (Section 3.2) essentially approximates the exact temperature profiles in each phase by linear temperature gradients.

The two approaches are formulated below and results from the approaches are compared with the exact solution in Section 5.

3.1 The Amateur Mathematician approach

This approach essentially replaces expressions involving error functions with polynomial functions in the energy equations. The resulting equations for λ_1 and λ_2 are quadratics, which can be easily solved. The approach makes use of formulae described in Appendix A.

Phase change criteria

The exact expressions are equations (2.32) and (2.33); the phase change constants are obtained by solving an equation with the following form:

$$\frac{e^{-\lambda^2}}{\mathrm{erf}(\lambda)} - \frac{e^{-c^2\lambda^2}}{\mathrm{erfc}(c\lambda)} \times d - \lambda \times e = 0 \tag{3.1}$$

where c, d and e are constants which differ according to which equation, (2.32) or (2.33), is being solved and λ is either λ_1 or λ_2.

To solve for λ approximate functions (A-11) and (A-14) are substituted into equation (3.1) to obtain a quadratic equation:

$$\left(e + 1.35 \times c \times d + \sqrt{\pi}/3\right) \times \lambda^2 + d \times \lambda - \sqrt{\pi}/2 = 0 \tag{3.2}$$

Equation (3.2) can be solved without iteration. The phase change conditions can therefore be obtained by solving equation (3.2) for λ_1 and λ_2 respectively, and substituting the answer into equation (2.32) or (2.33).

Case of liquid freezing; no structure melting

The exact expression is equation (2.10); λ_1 is obtained by solving a equation with the following form:

$$\frac{a\times e^{-\lambda_1^2}}{(1+a\times \mathrm{erf}(\lambda_1))}\times f-\frac{e^{-c^2\lambda_1^2}}{\mathrm{erfc}(c\lambda_1)}\times d-\lambda_1\times e=0 \qquad (3.3)$$

where a, c, d, e and f are constants which can be identified from equation (2.10).

Approximate functions (A-11) and (A-16) are substituted into equation (3.3) to obtain a cubic equation in λ_1:

$$\frac{(e+1.35cd)}{3}\times\lambda_1^3+\left(\frac{d}{3}+\frac{2af}{3}+\frac{2a}{\pi^{1/2}}(e+1.35cd)\right)\times\lambda_1^2 + \left(e+1.35cd+\frac{2ad}{\pi^{1/2}}\right)\times\lambda_1+(d-af)=0 \qquad (3.4)$$

Equation (3.4) cannot be solved directly unless the term in λ_1^3 is small compared with the term containing λ_1. This is in fact true and so the term in λ_1^3 is neglected. λ_1 can then be obtained from the resulting quadratic:

$$\left(\frac{d}{3}+\frac{2af}{3}+\frac{2a}{\pi^{1/2}}(e+1.35cd)\right)\times\lambda_1^2+\left(e+1.35cd+\frac{2ad}{\pi^{1/2}}\right)\times\lambda_1+(d-af)=0 \qquad (3.5)$$

The resulting interface temperatures and fuel heat losses are then obtained by substituting λ_1 into equations (2.9) and (2.12). (The error function is evaluated using formula (A-7) in Appendix A.)

Case of simultaneous liquid freezing and structure melting

The exact expressions are equation (2.25); λ_1 and λ_2 are obtained by solving two equations with the following form:

$$\frac{a\times e^{-\lambda^2}}{(b+a\times \mathrm{erf}(\lambda))}-\frac{e^{-c^2\lambda^2}}{\mathrm{erfc}(c\lambda)}\times d-\lambda\times e=0 \qquad (3.6)$$

where a, c, d and e are constants which can be identified from equation (2.25). Constant b is dependent on the value of the value of the other λ, and so the pair of equations (2.25) strictly need to be solved simultaneously to obtain consistent values of λ_1 and λ_2. However a reasonable approximation is to solve the equation for λ_2 first, using an estimate for λ_1 (a value $\mathrm{erf}(\lambda_1)=0.67$ was chosen), and the resulting estimate of λ_2 is fed back into the equation for λ_1.

To solve equation (3.6), approximate functions (A-11) and (A-16) are substituted to obtain the following cubic equation in λ:

$$\frac{(e+1.35cd)}{3}\times\lambda^3+\left(\frac{d}{3}+\frac{2a}{3b}+\frac{2a}{\pi^{1/2}b}(e+1.35cd)\right)\times\lambda^2 + \left(e+1.35cd+\frac{2ad}{\pi^{1/2}b}\right)\times\lambda+\left(d-\frac{a}{b}\right)=0 \qquad (3.7)$$

Equation (3.7) cannot be solved directly unless the term in λ^3 is small compared with the term containing λ. This is in fact true and so the term in λ^3 is neglected. λ can then be obtained from the resulting quadratic:

$$\left(\frac{d}{3}+\frac{2a}{3b}+\frac{2a}{\pi^{1/2}b}(e+1.35cd)\right)\times\lambda^2+\left(e+1.35cd+\frac{2ad}{\pi^{1/2}b}\right)\times\lambda+\left(d-\frac{a}{b}\right)=0 \qquad (3.8)$$

Having obtained λ_1 and λ_2 using equation (3.8) the resulting interface temperatures and fuel heat losses are then evaluated by substituting λ_1 into equations (2.24), (2.28) and (2.29). (The error function is evaluated using formula (A-7) in Appendix A.)

3.2 The Naive Physicist approach

This approach essentially approximates the exact temperature profiles in the phases by linear temperature gradients. The temperature gradients in the case of simultaneous liquid freezing/structure melting are illustrated in Figure 3. The solidification and melting constants are then obtained from a simplified energy conservation equation.

Case of simultaneous liquid freezing and structure melting

Figure 3 shows how the phases are distinguished for the case of simultaneous melting and freezing. The penetration length of the thermal front in the liquid is $2\sqrt{\alpha_{1,l}t}$. The solidification front is $|X_1|=2\lambda_1\sqrt{\alpha_{1,s}t}$. The melting front in the structure is $|X_2|=2\lambda_2\sqrt{\alpha_{2,l}t}$, whilst the penetration length of the thermal front in the structure is $2\sqrt{\alpha_{2,s}t}$.

The energy balance for the material 1 phases at time T gives:

$$\int_0^T q_{1,t}dt = -\int_0^T k_{1,s}\left.\frac{\partial T_{1,s}}{\partial x}\right|_{x=0} dt = \frac{\omega_{1,s}}{\lambda_1}.\left(T_{1,mp} - T_i\right).\sqrt{T}$$

$$\int_0^T q_{1,l}dt = 2\left(\sqrt{\alpha_{1,l}T} - \lambda_1\sqrt{\alpha_{1,s}T}\right).c_{1,l}\rho_1.\left(T_{1,\infty} - \overline{T}_{1,l}\right) + 2\lambda_1\sqrt{\alpha_{1,s}T}.c_{1,l}\rho_1.\Delta T_1$$

$$= \left(1+\beta_1\lambda_1\right)\omega_{1,l}\Delta T_1\sqrt{T}$$

$$\int_0^T q_{1,L}dt = L_1\rho_1 \times 2\lambda_1\sqrt{\alpha_{1,s}T} = \frac{2\omega_{1,s}L_1\lambda_1}{c_{1,s}}\sqrt{T} \qquad (3.9)$$

$$\int_0^T q_{1,s}dt = 2\lambda_1\sqrt{\alpha_{1,s}T}.c_{1,s}\rho_1.\left(T_{1,mp} - \overline{T}_{1,s}\right) = \omega_{1,s}\lambda_1\left(T_{1,mp} - T_i\right)\sqrt{T}$$

The energy balance for the material 2 phases at time T gives:

$$\int_0^T q_{2,t}dt = -\int_0^T k_{2,l}\left.\frac{\partial T_{2,l}}{\partial x}\right|_{x=0} dt = \frac{\omega_{2,l}}{\lambda_2}.\left(T_i - T_{2,mp}\right).\sqrt{T}$$

$$\int_0^T q_{2,l}dt = 2\lambda_2\sqrt{\alpha_{2,l}T}.c_{2,l}\rho_2.\left(\overline{T}_{2,l} - T_{2,mp}\right) = \omega_{2,l}\lambda_2\left(T_i - T_{2,mp}\right)\sqrt{T}$$

$$\int_0^T q_{2,L}dt = L_2\rho_2 \times 2\lambda_2\sqrt{\alpha_{2,l}T} = \frac{2\omega_{2,l}L_2\lambda_2}{c_{2,l}}\sqrt{T} \qquad (3.10)$$

$$\int_0^T q_{2,s}dt = 2\left(\sqrt{\alpha_{2,s}T} - \lambda_2\sqrt{\alpha_{2,l}T}\right).c_{2,s}\rho_2.\left(\overline{T}_{2,s} - T_{2,\infty}\right) + 2\lambda_2\sqrt{\alpha_{2,l}T}.c_{2,s}\rho_2.\Delta T_2$$

$$= \left(1+\beta_2\lambda_2\right)\omega_{2,s}\Delta T_2\sqrt{T}$$

The interface temperature is obtained by equating the heat flux at the interface:

$$T_i = \frac{\left(\omega_{1,s}/\lambda_1\right) \times T_{1,mp} + \left(\omega_{2,l}/\lambda_2\right) \times T_{2,mp}}{\left(\omega_{1,s}/\lambda_1 + \omega_{2,l}/\lambda_2\right)} \qquad (3.11)$$

The interface temperature expressed by equation (3.11) differs from the exact solution (equation (2.24)). The energy equations for the two materials are:

$$\int_0^T q_{1,l}dt + \int_0^T q_{1,L}dt + \int_0^T q_{1,s}dt = \int_0^T q_{1,t}dt$$

$$\int_0^T q_{2,l}dt + \int_0^T q_{2,L}dt + \int_0^T q_{2,s}dt = \int_0^T q_{2,t}dt \qquad (3.12)$$

Substituting equation (3.9) into equation (3.12), and rearranging terms, yields a quadratic equation in λ_1:

$$\left(1+\frac{2\Lambda_1}{\pi^{1/2}}+\beta_1\frac{\omega_{1,l}}{\omega_{1,s}}\frac{\Delta T_1}{\Delta T_{mp}}\right)\times\lambda_1^2+\left(\frac{\omega_{1,s}}{\omega_{2,l}}\frac{2\Lambda_1\lambda_2}{\pi^{1/2}}+\left(\frac{\omega_{1,l}}{\omega_{1,s}}+\beta_1\lambda_2\frac{\omega_{1,l}}{\omega_{2,l}}\right).\frac{\Delta T_1}{\Delta T_{mp}}\right)\times\lambda_1 + \left(\lambda_2\frac{\omega_{1,l}}{\omega_{2,l}}\frac{\Delta T_1}{\Delta T_{mp}}-1\right)=0 \tag{3.13}$$

Similarly, substituting equation (3.10) into equation (3.12), and rearranging terms, yields a quadratic equation in λ_2:

$$\left(1+\frac{2\Lambda_2}{\pi^{1/2}}+\beta_2\frac{\omega_{2,s}}{\omega_{2,l}}\frac{\Delta T_2}{\Delta T_{mp}}\right)\times\lambda_2^2+\left(\frac{\omega_{2,l}}{\omega_{1,s}}\frac{2\Lambda_2\lambda_1}{\pi^{1/2}}+\left(\frac{\omega_{2,s}}{\omega_{2,l}}+\beta_2\lambda_1\frac{\omega_{2,s}}{\omega_{1,s}}\right).\frac{\Delta T_2}{\Delta T_{mp}}\right)\times\lambda_2 + \left(\lambda_1\frac{\omega_{2,s}}{\omega_{1,s}}\frac{\Delta T_2}{\Delta T_{mp}}-1\right)=0 \tag{3.14}$$

The terms in equations (3.13) and (3.14) are similar, but not quite identical, to the quadratic solutions obtained by the Amateur Mathematician approach (equation (3.8)). The similarity is encouraging since it indicates that the simple Naive Physicist approach yields functions which approximate the functions in the exact solution.

Equations (3.13) and (3.14) should strictly be solved iteratively to obtain consistent values of λ_1 and λ_2. However to avoid iteration the same method used in the Amateur Mathematician approach is adopted: equation (3.14) for λ_2 is solved first, using an estimate for λ_1 (a value $\lambda_1=0.67$ was chosen) and the resulting estimates of λ_2 are fed back into the equation for λ_1.

Once λ_1 and λ_2 have been obtained the heat losses and gains in the various phases are evaluated using the following equations:

$$\begin{aligned}
Q_{1,l} &= (1+\beta_1\lambda_1).\omega_{1,l}.\left(\lambda_1/\omega_{1,s}+\lambda_2/\omega_{2,l}\right).\frac{\Delta T_1}{\Delta T_{mp}} \\
Q_{1,L} &= \frac{2\Lambda_1\lambda_1}{\pi^{1/2}}.\left(\lambda_1+\frac{\omega_{1,s}}{\omega_{2,l}}\lambda_2\right) \\
Q_{1,s} &= \lambda_1^2
\end{aligned} \tag{3.15}$$

$$\begin{aligned}
Q_{2,l} &= \lambda_2^2 \\
Q_{2,L} &= \frac{2\Lambda_2\lambda_2}{\pi^{1/2}}.\left(\lambda_2+\frac{\omega_{2,l}}{\omega_{1,s}}\lambda_1\right) \\
Q_{2,s} &= (1+\beta_2\lambda_2).\omega_{2,s}.\left(\lambda_2/\omega_{2,l}+\lambda_1/\omega_{1,s}\right).\frac{\Delta T_2}{\Delta T_{mp}}
\end{aligned} \tag{3.16}$$

Equations (3.15) and (3.16) resemble the exact solutions (2.28) and (2.29).

The Naive Physicist approach does not involve evaluating the error function, and the equations are much simpler than the exact solutions.

Case of liquid freezing; no structure melting

This case is a trivial extension of the case of simultaneous freezing/melting since it is necessary only to neglect the molten structure layer and set $\lambda_2 = 0$. The energy balance for the material 1 phases is unaltered.

The energy balance for material 2 is simply:

$$\int_0^T q_{2,t}dt = \int_0^T q_{2,s}dt = \omega_{2,s}.\left(T_i - T_{2,\infty}\right).\sqrt{T} \tag{3.17}$$

The interface temperature is obtained by equating the heat flux at the interface:

$$T_i = \frac{\left(\omega_{1,s}/\lambda_1\right)\times T_{1,mp} + \omega_{2,s}\times T_{2,\infty}}{\left(\omega_{1,s}/\lambda_1 + \omega_{2,s}\right)} \tag{3.18}$$

Substituting equation (3.18) into equation (3.12), and rearranging terms, yields a quadratic equation in λ_1:

$$\left(\left(1+\frac{\Delta T_2}{\Delta T_{mp}}\right)+\frac{2\Lambda_1}{\pi^{1/2}}+\beta_1\frac{\omega_{1,l}}{\omega_{1,s}}\frac{\Delta T_1}{\Delta T_{mp}}\right)\times\lambda_1^2+\left(\frac{\omega_{1,s}}{\omega_{2,s}}\frac{2\Lambda_1}{\pi^{1/2}}+\left(\frac{\omega_{1,l}}{\omega_{1,s}}+\beta_1\frac{\omega_{1,l}}{\omega_{2,s}}\right).\frac{\Delta T_1}{\Delta T_{mp}}\right)\times\lambda_1 + \left(\frac{\omega_{1,l}}{\omega_{2,s}}\frac{\Delta T_1}{\Delta T_{mp}}-\left(1+\frac{\Delta T_2}{\Delta T_{mp}}\right)\right)=0 \tag{3.19}$$

Once λ_1 has been obtained the heat losses and gains in the material 1 phases are evaluated using the following equations:

$$Q_{1,l} = \left(1+\beta_1\lambda_1\right).\omega_{1,l}.\left(\lambda_1/\omega_{1,s} + 1/\omega_{2,s}\right).\frac{\Delta T_1}{\left(\Delta T_{mp}+\Delta T_2\right)}$$

$$Q_{1,L} = \frac{2\Lambda_1\lambda_1}{\pi^{1/2}}.\left(\lambda_1+\frac{\omega_{1.s}}{\omega_{2,l}}\right).\frac{1}{\left(1+\Delta T_2/\Delta T_{mp}\right)} \tag{3.20}$$

$$Q_{1,s} = \lambda_1^2$$

Phase change criteria

The criterion for structure melting is obtained by setting $\lambda_2 = 0$ in equations (3.13) and (3.14). The resulting pair of equations are:

$$\frac{\Delta T_2}{\Delta T_{mp}} = \frac{\omega_{1,s}}{\omega_{2,s}\lambda_1} \quad \text{and}$$
$$\left(1 + \frac{2\Lambda_1}{\pi^{1/2}} + \beta_1 \frac{\omega_{1,l}}{\omega_{1,s}} \frac{\Delta T_1}{\Delta T_{mp}}\right) \times \lambda_1^2 + \left(\frac{\omega_{1,l}}{\omega_{1,s}} . \frac{\Delta T_1}{\Delta T_{mp}}\right) \times \lambda_1 - 1 = 0 \qquad (3.21)$$

The criterion for liquid freezing is obtained by setting $\lambda_1 = 0$ in equations (3.13) and (3.14). The resulting pair of equations are:

$$\frac{\Delta T_1}{\Delta T_{mp}} = \frac{\omega_{2,l}}{\omega_{1,l}\lambda_2} \quad \text{and}$$
$$\left(1 + \frac{2\Lambda_2}{\pi^{1/2}} + \beta_2 \frac{\omega_{2,s}}{\omega_{2,l}} \frac{\Delta T_2}{\Delta T_{mp}}\right) \times \lambda_2^2 + \left(\frac{\omega_{2,s}}{\omega_{2,l}} . \frac{\Delta T_2}{\Delta T_{mp}}\right) \times \lambda_2 - 1 = 0 \qquad (3.22)$$

3.3 Summary

Two approximate approaches have been developed to estimate the key quantities when either a hot liquid or a cold structure undergo phase change at a surface. The approaches essentially simplify the energy equations in the two materials as quadratic functions. This avoids the iteration procedure which is necessary to obtain an exact solution, and enables a direct solution to be obtained. The approaches are compared with the exact solution in Section 5.

The Naive Physicist approach, described in Section 3.2, is particularly interesting because it calculates transient crust growth using a model which assumes single-node temperatures in all the phases. This assumption is essentially used in SIMMER-III to compute the growth of fuel crust on structure. The comparison of results using the Naive Physicist approach with the exact solution provides an indication of the suitability of a single-temperature node representation of the crust.

4. FORMULATION FOR AN IDEALIZED INTERFACIAL GAP

4.1 Description of the gap

When a melt makes contact with structure, the melt-structure contact is not necessarily perfect. In particular the freezing behaviour of UO_2 melt penetrating steel-walled tubes has been interpreted only by postulating a melt-wall gap [4]. Furthermore even after a crust forms, differential thermal expansion can cause a gap to form between the crust and the structure. The effect of the gap is to introduce a thermal resistance between material 1 and material 2 in the formulation described in Section 2.

The interface thermal resistance is treated as a gap heat transfer coefficient, h, which transfers heat between two interface temperatures, $T_{i,1}$ and $T_{i,2}$, which bound the gap:

$$q = h.\left(T_{i,1} - T_{i,2}\right) \tag{4.1}$$

Equation (4.1) introduces three new variables: h, $T_{i,1}$ and $T_{i,2}$. In Section 2 it was shown that the heat flux transferred from material 1 to material 2 decays according to $1/t^{1/2}$. Equation (4.1) shows that a time-variant heat flux q implies interface temperatures and/or a gap conductance which vary with time.

In this analysis the interface temperatures $T_{i,1}$ and $T_{i,2}$ are assumed to be time-invariant. To reproduce the transient heat fluxes, the gap conductance which varies according to $1/t^{1/2}$ is assumed. The heat flux through the interface resistance is:

$$q_{1,t} = -k_{1,s}\left.\frac{\partial T_{1,s}}{\partial x}\right|_{x=0} = \frac{h_g}{\sqrt{\pi t}}.\left(T_{i,1} - T_{i,2}\right) = q_{2,t} \tag{4.2}$$

where the gap conductance h_g is a constant. This formulation of the gap thermal resistance is of course ideal, but it is the only form of gap conductance which can be solved using the methods developed in Section 2.

In Section 4.2 the gap conductance defined by equation (4.2) is used to show how a transient interface resistance alters the formulae derived in Sections 2. The boundary conditions used in Section 2 also apply in this section, with the exception that the temperature is discontinuous at x=0; the former single interface temperature T_i is replaced by a liquid-side interface temperature $T_{i,1}$ and a structure-side interface temperature $T_{i,2}$. The additional boundary conditions required at the interface are supplied by equation (4.2).

4.2 Effect of a transient gap conductance on interface temperatures and heat fluxes

Neither material undergoes phase change

The liquid-side interface temperature, formerly equation (2.5), becomes:

$$T_{i,1} = \frac{\omega_{1,l}\left(h_g + \omega_{2,s}\right) \times T_{1,\infty} + \omega_{2,s} h_g \times T_{2,\infty}}{\left(\omega_{1,l} h_g + \omega_{1,l}\omega_{2,s} + \omega_{2,s} h_g\right)} \tag{4.3}$$

The structure-side interface temperature, formerly equation (2.5), becomes:

$$T_{i,2} = \frac{\omega_{1,l} h_g \times T_{1,\infty} + \omega_{2,s}\left(h_g + \omega_{1,l}\right) \times T_{2,\infty}}{\left(\omega_{1,l} h_g + \omega_{1,l}\omega_{2,s} + \omega_{2,s} h_g\right)} \tag{4.4}$$

The heat flux from material 1 to material 2 is:

$$q_t = \frac{\left(T_{1,\infty} - T_{2,\infty}\right)}{\left(\frac{1}{\omega_{1,l}} + \frac{1}{h_g} + \frac{1}{\omega_{2,s}}\right)} \cdot \frac{1}{\sqrt{\pi t}} \tag{4.5}$$

These formulae are identical to those derived in Section 2.2 if the interface resistance is added in series to the liquid thermal resistance and the interface temperature is taken to be the structure-side interface temperature:

$$\frac{1}{\omega_{1,l}} \rightarrow \frac{1}{\omega_{1,l}} + \frac{1}{h_g}, \qquad T_i \rightarrow T_{i,2} \tag{4.6}$$

Liquid material 1 freezes, but solid material 2 does not melt

The liquid-side interface temperature, formerly equation (2.9), becomes:

$$T_{i,1} = \frac{\omega_{1,s}\left(h_g + \omega_{2,s}\right) \Big/ \mathrm{erf}(\lambda_1) \times T_{1,mp} + \omega_{2,s} h_g \times T_{2,\infty}}{\left(\omega_{1,s} h_g \Big/ \mathrm{erf}(\lambda_1) + \omega_{1,s}\omega_{2,s} \Big/ \mathrm{erf}(\lambda_1) + \omega_{2,s} h_g\right)} \tag{4.7}$$

The structure-side interface temperature, formerly equation (2.9), becomes:

$$T_{i,2} = \frac{\omega_{1,s} h_g \Big/ \mathrm{erf}(\lambda_1) \times T_{1,mp} + \omega_{2,s}\left(h_g + \omega_{1,s} \Big/ \mathrm{erf}(\lambda_1)\right) \times T_{2,\infty}}{\left(\omega_{1,s} h_g \Big/ \mathrm{erf}(\lambda_1) + \omega_{1,s}\omega_{2,s} \Big/ \mathrm{erf}(\lambda_1) + \omega_{2,s} h_g\right)} \tag{4.8}$$

The solidification constant for material 1, formerly equation (2.10), becomes:

$$\frac{\omega_{2,s}h_g e^{-\lambda_1^2}}{\left(\omega_{1,s}h_g+\omega_{1,s}\omega_{2,s}+\omega_{2,s}h_g\mathrm{erf}(\lambda_1)\right)}\cdot\frac{\left(\Delta T_{mp}+\Delta T_2\right)}{\Delta T_{mp}}-\frac{e^{-\beta_1^2\lambda_1^2}}{\mathrm{erfc}(\beta_1\lambda_1)}\cdot\frac{\omega_{1,l}}{\omega_{1,s}}\cdot\frac{\Delta T_1}{\Delta T_{mp}}=\Lambda_1\lambda_1 \qquad (4.9)$$

The expressions for the heat flux from liquid and the latent heat liberated by freezing fuel are unaltered from equation (2.11). However the total heat transfer from material 1 to material 2, and the net heat flux from the crust become:

$$q_{l,t}=\frac{\omega_{1,s}\omega_{2,s}h_g}{\left(\omega_{1,s}h_g+\omega_{1,s}\omega_{2,s}+\omega_{2,s}h_g\mathrm{erf}(\lambda_1)\right)}\cdot\frac{\left(\Delta T_{mp}+\Delta T_2\right)}{\sqrt{\pi t}}$$
$$q_{l,s}=\frac{\omega_{1,s}\omega_{2,s}h_g\left(1-e^{-\lambda_1^2}\right)}{\left(\omega_{1,s}h_g+\omega_{1,s}\omega_{2,s}+\omega_{2,s}h_g\mathrm{erf}(\lambda_1)\right)}\cdot\frac{\left(\Delta T_{mp}+\Delta T_2\right)}{\sqrt{\pi t}} \qquad (4.10)$$

These formulae are identical to those derived in Section 2.3 if the interface resistance is added in series to the crust thermal resistance and the interface temperature is taken to be the structure-side interface temperature:

$$\frac{\mathrm{erf}(\lambda_1)}{\omega_{1,s}}\rightarrow\frac{\mathrm{erf}(\lambda_1)}{\omega_{1,s}}+\frac{1}{h_g},$$
$$T_i\rightarrow T_{i,2} \qquad (4.11)$$

Simultaneous freezing of liquid 1 and melting of solid 2

The liquid-side interface temperature, formerly equation (2.24), becomes:

$$T_{i,1}=\frac{\omega_{1,s}/\mathrm{erf}(\lambda_1)\times\left(h_g+\omega_{2,l}/\mathrm{erf}(\lambda_2)\right)\times T_{1,mp}+\omega_{2,l}h_g/\mathrm{erf}(\lambda_2)\times T_{2,mp}}{\left(\omega_{1,s}h_g/\mathrm{erf}(\lambda_1)+\omega_{1,s}\omega_{2,l}/\mathrm{erf}(\lambda_1)\mathrm{erf}(\lambda_2)+\omega_{2,l}h_g/\mathrm{erf}(\lambda_2)\right)} \qquad (4.12)$$

The structure-side interface temperature, formerly equation (2.24), becomes:

$$T_{i,2}=\frac{\omega_{1,s}h_g/\mathrm{erf}(\lambda_1)\times T_{1,mp}+\omega_{2,l}/\mathrm{erf}(\lambda_2)\times\left(h_g+\omega_{1,s}/\mathrm{erf}(\lambda_1)\right)\times T_{2,mp}}{\left(\omega_{1,s}h_g/\mathrm{erf}(\lambda_1)+\omega_{1,s}\omega_{2,l}/\mathrm{erf}(\lambda_1)\mathrm{erf}(\lambda_2)+\omega_{2,l}h_g/\mathrm{erf}(\lambda_2)\right)} \qquad (4.13)$$

The solidification and melting constants, formerly equation (2.25), become:

$$\frac{\omega_{2,l}h_g e^{-\lambda_1^2}}{\left(\omega_{2,l}h_g\mathrm{erf}(\lambda_1)+\omega_{1,s}h_g\mathrm{erf}(\lambda_2)+\omega_{1,s}\omega_{2,l}\right)}-\frac{e^{-\beta_1^2\lambda_1^2}}{\mathrm{erfc}(\beta_1\lambda_1)}\cdot\frac{\omega_{1,l}}{\omega_{1,s}}\cdot\frac{\Delta T_1}{\Delta T_{mp}}=\Lambda_1\lambda_1$$
$$\frac{\omega_{1,s}h_g e^{-\lambda_2^2}}{\left(\omega_{2,l}h_g\mathrm{erf}(\lambda_1)+\omega_{1,s}h_g\mathrm{erf}(\lambda_2)+\omega_{1,s}\omega_{2,l}\right)}-\frac{e^{-\beta_2^2\lambda_2^2}}{\mathrm{erfc}(\beta_2\lambda_2)}\cdot\frac{\omega_{2,s}}{\omega_{2,l}}\cdot\frac{\Delta T_2}{\Delta T_{mp}}=\Lambda_2\lambda_2 \qquad (4.14)$$

The expressions for the heat flux from liquid and the latent heat liberated by freezing of material 1 are unaltered from equation (2.26). However the total heat flux from material 1 to material 2, and the net heat flux from the crust become:

$$q_{1,t} = \frac{\omega_{1,s}\omega_{2,l}h_g}{\left(\omega_{1,s}h_g\mathrm{erf}(\lambda_2)+\omega_{1,s}\omega_{2,s}+\omega_{2,l}h_g\mathrm{erf}(\lambda_1)\right)}\cdot\frac{\Delta T_{mp}}{\sqrt{\pi t}}$$

$$q_{1,s} = \frac{\omega_{1,s}\omega_{2,l}h_g\left(1-e^{-\lambda_1^2}\right)}{\left(\omega_{1,s}h_g\mathrm{erf}(\lambda_2)+\omega_{1,s}\omega_{2,s}+\omega_{2,l}h_g\mathrm{erf}(\lambda_1)\right)}\cdot\frac{\Delta T_{mp}}{\sqrt{\pi t}} \qquad (4.15)$$

The expressions for the heat flux to structure and the latent heat absorbed by melting structure are unaltered from equation (2.27). However the total heat flux from material 1 to material 2, and the net heat flux to the liquid structure become:

$$q_{2,t} = \frac{\omega_{1,s}\omega_{2,l}h_g}{\left(\omega_{1,s}h_g\mathrm{erf}(\lambda_2)+\omega_{1,s}\omega_{2,s}+\omega_{2,l}h_g\mathrm{erf}(\lambda_1)\right)}\cdot\frac{\Delta T_{mp}}{\sqrt{\pi t}}$$

$$q_{2,l} = \frac{\omega_{1,s}\omega_{2,l}h_g\left(1-e^{-\lambda_2^2}\right)}{\left(\omega_{1,s}h_g\mathrm{erf}(\lambda_2)+\omega_{1,s}\omega_{2,s}+\omega_{2,l}h_g\mathrm{erf}(\lambda_1)\right)}\cdot\frac{\Delta T_{mp}}{\sqrt{\pi t}} \qquad (4.16)$$

These formulae are identical to those derived in Section 2.5 if the interface resistance is added in series to the crust thermal resistance and the interface temperature is taken to be the structure-side interface temperature.

4.3 Effect of a transient gap conductance on phase change criteria

The criteria for the freezing of material 1 and the melting of material 2 which were established in Section 2 are complicated by the introduction of a gap conductance. The criterion for freezing of material 1 is that the liquid-side interface temperature $T_{i,l}$ is below the equilibrium melting temperature of material 1. Conversely the criterion for melting of material 2 is that the structure-side interface temperature $T_{i,2}$ is above the equilibrium melting temperature of material 2. Furthermore the presence of an interface resistance makes it possible for the condition of no freezing and no melting to be achieved since $T_{i,l}$ can be above the melting point of material 1 and $T_{i,2}$ can simultaneously be below the structure melting point.

The effect of a gap conductance on the phase change map of the UO_2-steel system (Figure 5) is important: the number of possible phase change combinations increases from three (liquid UO_2 freezing only; UO_2 freezing and steel structure melting; steel structure melting only) to four (all the former plus no freezing nor melting). On the phase change map the four regions meet at a single point, which is christened the "quadruple point" or "quad point" for brevity. The four lines radiating from the quad point define the boundaries of the different phase change regions.

The Quad point

The quad point is obtained by setting $\lambda_1 = 0$ and $\lambda_2 = 0$ in equation (4.14):

$$\frac{\Delta T_2}{\Delta T_{mp}} = \frac{h_g}{\omega_{2,s}}$$
$$\frac{\Delta T_1}{\Delta T_{mp}} = \frac{h_g}{\omega_{1,l}} \qquad (4.17)$$

Condition for material 1 freezing when material 2 is not melting

The boundary for freezing of material 1 without structure melting is obtained by setting $T_{i,1} = T_{1,mp}$ in equation (4.6):

$$\Delta T_1 = \frac{\omega_{2,s} h_g}{\omega_{1,l}\left(h_g + \omega_{2,s}\right)}\left(\Delta T_{mp} + \Delta T_2\right) \qquad (4.18)$$

Condition for material 2 melting when material 1 is not freezing

The boundary for structure melting without freezing of material 1 is obtained by setting $T_{i,2} = T_{2,mp}$ in equation (4.7):

$$\Delta T_2 = \frac{\omega_{1,l} h_g}{\omega_{2,s}\left(h_g + \omega_{1,l}\right)}\left(\Delta T_{mp} + \Delta T_1\right) \qquad (4.19)$$

Condition for material 1 freezing when material 2 is melting

The boundary for freezing of material 1 simultaneously with structure melting is obtained by setting $\lambda_1 = 0$ in equation (4.14):

$$\frac{\Delta T_1}{\Delta T_{mp}} = \frac{1}{\omega_{1,l}\left(\dfrac{\mathrm{erf}(\lambda_2)}{\omega_{2,l}} + \dfrac{1}{h_g}\right)}$$
$$\frac{e^{-\lambda_2^2}}{\left(\mathrm{erf}(\lambda_2) + \omega_{2,l}/h_g\right)} - \frac{e^{-\beta_2^2\lambda_2^2}}{\mathrm{erfc}(\beta_2\lambda_2)} \cdot \frac{\omega_{2,s}}{\omega_{2,l}} \cdot \frac{\Delta T_2}{\Delta T_{mp}} = \Lambda_2\lambda_2 \qquad (4.20)$$

Condition for material 2 melting when material 1 is freezing

The boundary for structure melting when material 1 is freezing is obtained by setting $\lambda_2 = 0$ in equation (4.14):

$$\frac{\Delta T_2}{\Delta T_{mp}} = \frac{1}{\omega_{2,s}\left(\frac{\mathrm{erf}(\lambda_1)}{\omega_{1,s}} + \frac{1}{h_g}\right)}$$

$$\frac{e^{-\lambda_1^2}}{\left(\mathrm{erf}(\lambda_1) + \omega_{1,s}/h_g\right)} - \frac{e^{-\beta_1^2\lambda_1^2}}{\mathrm{erfc}(\beta_1\lambda_1)} \cdot \frac{\omega_{1,l}}{\omega_{1,s}} \cdot \frac{\Delta T_1}{\Delta T_{mp}} = \Lambda_1\lambda_1 \qquad (4.21)$$

4.4 Summary

Solutions to the transient heat conduction equations which include an idealized gap heat transfer coefficient (equation (4.2)) are described. The solutions are equivalent to the solutions obtained in Section 2 by letting $h_g \to \infty$. A gap conductance can significantly alter phase change criteria; the phase change map for the UO_2-steel system is described in Section 5.

5. RESULTS FOR LIQUID UO_2 IN CONTACT WITH SOLID STEEL

The melting temperature of UO_2 is 3120 K. The steel melting temperature is taken in this report to be 1733 K, which lies mid-way between the solidus (1713 K) and liquidus (1753 K) temperatures. Therefore when liquid UO_2 makes contact with solid steel a phase change must occur, if equilibrium phase change conditions are assumed, since the interface temperature must lie either below the fuel melting temperature or above the steel melting temperature. When the initial steel temperature is low the only phase change which occurs is freezing of UO_2 to form a crust; at high initial temperatures both UO_2 freezing and steel melting occur.

Results have been obtained using a small computer program, called "Meltit". Meltit allows calculations to be quickly repeated using different values for variables and materials properties. The program is briefly described in Section 5.1, and results obtained using the exact solutions of Section 2 are described in Section 5.2. A comparison of the approximate solutions of Section 3 with the exact solution is performed in Section 5.3, and the effect of a gap thermal resistance is illustrated in Section 5.4. In the following sections UO_2 is frequently referred to as "fuel" for shorthand.

The materials properties used in the calculations are obtained from the latest SIMMER-III equation-of-state and thermophysical properties database [3]. In particular the liquid UO_2 thermal conductivity is 2.5 W/m/K, and polynomial functions have been fitted to the specific heat capacities at constant pressure of the liquids. The steel solid specific heat is in fact discontinuous at 1200 K, but it has been approximated by a smooth function to avoid discontinuity in the calculated results. The materials properties are detailed in Appendix B.

5.1 Meltit: A computer program for calculating key heat conduction results

The Meltit program consists of about 2000 lines and currently resides in the following directory on a RSS workstation:

/user9/djb/meltit

The directory contains a run script and the program contains a description of the output streams.

Meltit consists of a main program, which calculates the results for a matrix of liquid UO_2 and solid steel temperatures (see Table B.1 of Appendix B for the array used), and several subroutines which are called by the main program to perform specific operations. The subroutines are:

matopt To calculate materials properties using the equations listed in Appendix B. Changes to materials properties are confined to this routine.

erf To calculate the error function using equation (A-6) of Appendix A. The values of the error function by this method are in agreement with tabulated values to within at least four significant figures.

erfinv To calculate the inverse error function using Newton-Raphson iterations and equation (A-6).

flamb To solve for λ in the following function using the Newton-Raphson method (a, b, c, d, e and f are constants):

$$\frac{a \times e^{-\lambda^2}}{(b + a \times \mathrm{erf}(\lambda))} \times f - \frac{e^{c^2\lambda^2}}{\mathrm{erfc}(c\lambda)} \times d - \lambda \times e = 0 \qquad (5.1)$$

Results are calculated assuming that materials properties for each phase (solid and liquid UO_2, solid and liquid steel) are constant. The properties are evaluated in subroutine *matopt* at one reference temperature for each phase. The choice of reference temperature is a source of uncertainty since, for example, the solid steel temperature can vary spatially between its initial temperature and the steel melting temperature, with a consequent large variation of materials properties. Three options to specify the reference temperature are available, as illustrated in Figure 4:

(a) Method 1 (M1). The UO_2 properties are calculated at the UO_2 melting point; the steel properties are calculated at the steel melting point. Constant materials properties are used to perform all the calculations.

(b) Method 2 (M2). Liquid UO_2 and solid steel properties are calculated at their initial (bulk) temperatures, whilst solid UO_2 and liquid steel properties are calculated at their melting points, as per M1.

(c) Method 3 (M3). The properties of all phases are evaluated at their mid-point temperatures, as shown in Figure 4. This method is perhaps the best estimate of materials properties, but it also requires an extra iteration within the program since the interface temperature, which is required to establish the mid-point solid fuel and liquid steel temperatures, is not known at the start of the calculation.

case of simultaneous fuel freezing / steel melting

For each pair of liquid fuel and solid steel temperatures which satisfy the condition of simultaneous freezing/melting at the interface, the fuel and steel phase change constants, λ_1 and λ_2, are obtained by iteration from equation (2.25). The resulting interface temperature, heat fluxes and phase change fronts are evaluated from equations (2.24), (2.28), (2.29) and (2.31).

case of fuel freezing / no steel melting

For each pair of liquid fuel and solid steel temperatures which satisfy the condition of fuel freezing without steel melting at the interface, the fuel solidification constant is obtained from equation (2.10). The resulting interface temperature and heat fluxes are evaluated using equations (2.9) and (2.12).

solutions using approximate methods

The quantities using the approximate methods described in Section 3 are computed for comparison with results using the exact solution derived above.

gap conductance

The effect of a gap conductance on the phase change map is computed according to the formulation in Section 4.

5.2 Results using the exact solution for perfect contact

Results are presented using the three methods (M1 to M3) to determine materials properties described in Section 5.1. A further calculation, Method 3k (M3k), used a liquid fuel conductivity of 5.6 W/m/K instead of 2.5 W/m/K to investigate the effect of uncertainties in the thermal conductivity of liquid fuel.

The phase change map

The phase change map depicts the boundaries of the three conceivable phase change combinations: (a) fuel freezing without steel melting, (b) fuel freezing and simultaneous steel melting, and (c) steel melting without fuel freezing. The boundaries correspond to the two criteria of No Steel Melting and No Fuel Freezing. The criteria calculated using Methods M1 to M3k are shown in Figure 5, where the x-axis abscissa extends from 400 K to the steel melting point (1733 K) and the y-axis ordinate extends from the fuel melting point (3120 K) to 10000 K.

Although a phase change of steel melting without fuel freezing is conceivable, Figure 5 shows that it can occur only at unrealistically high fuel temperatures (above 7000 K), if at all. The case of no fuel freezing is therefore not discussed further in this report.

The criterion for No Steel Melting calculated by Method 3 indicates that liquid fuel close to its melting point induces steel melting for steel temperatures above about 1200 K. This is higher than the 900 K predicted by Epstein [1], but is more consistent with the analysis of Hayden [2]. The discrepancy is caused mainly by the use of solid steel properties at the initial steel temperature in the original analysis by Epstein; in particular the solid steel thermal conductivity is

underestimated by as much as a factor of 2. All Methods show that higher liquid fuel temperatures cause steel melting at lower steel temperatures.

The different methods used to calculate materials properties predict slightly different phase change boundaries. M3 and M3k diverge as the fuel temperature increases, due to the effect of the higher liquid fuel thermal conductivity in M3k. The discrepancy between M2 (which uses material properties at the initial temperatures) and the other methods is most pronounced and is caused by the much lower steel thermal conductivity and heat capacity at lower temperatures.

The criterion for No Steel Melting is compared against experimental data in Section 5.5. Nevertheless Figure 5 indicates the following points:

- The assumption that constant materials properties can be assigned to the four phases is only approximately valid for UO_2/steel. This is illustrated by the spread in results between Methods M1 to M3k. It is necessary to take into account the temperature-variation of steel properties, and to evaluate properties at a suitable reference temperature.

- The least accurate method for estimating the criterion for No Steel Melting is Method 2, which uses materials properties evaluated at the initial temperature. This is the method used by Epstein [1].

- The most accurate method for estimating the criterion for No Steel Melting is believed to be Method 3, since this uses a mid-point reference temperature for each phase. Method 3 is consistent with the calculations by Hayden [2].

The phase change constants

The phase change "constants", λ_1 and λ_2, obtained by Method 3 are plotted in Figures 6(a) and 6(b) respectively for a range of fuel and steel initial temperatures. Both phase change constants vary with the temperatures of the contacting materials. The value of the steel melting constant, λ_2, is sensitive to initial fuel and steel temperatures. The fuel solidification constant, λ_1, is fairly insensitive to the initial temperatures when the fuel temperature is less than about 3600 K. A suitable value for λ_1 in this temperature regime is ~ 0.7 to 0.8.

Fuel-steel interface temperature

The fuel-steel interface temperatures predicted by Method 3 are plotted in Figure 7(a) for a range of fuel and steel temperatures. Figure 7(a) shows that the value of the interface temperature is more sensitive to steel than to fuel temperature. Note that interface temperatures are predicted to be 1000 to 2000 K below the fuel melting temperature.

Interface temperatures calculated using all four Methods are plotted in Figures 8(a) to 8(c) for three fuel temperatures. The Methods tend to converge at higher steel temperature, although there remains a difference between Method 1 and Method 3, probably reflecting the variation in solid fuel thermal properties (particularly thermal conductivity and heat capacity). Method 2 diverges significantly at lower steel temperatures from the other methods, since it does not take into account the strong temperature-dependence of solid steel properties. The difference between methods M3 and M3k grows with higher fuel temperature.

The ratio of the steel liquid layer to the fuel crust thickness

The thickness of the liquid steel layer divided by the thickness of the fuel crust predicted by Method 3 is plotted in Figure 7(b) for a range of fuel and steel initial temperatures. When the ratio is unity, the molten steel layer and fuel crust are predicted to grow at the same rate.

Heat losses and gains

Heat is transferred from fuel to steel. The heat lost from the fuel comes from three sources: (a) cooling down of liquid fuel, (b) latent heat liberated by freezing, and (c) cooling down of solid fuel. The relative proportion of these sources to the total heat lost from the fuel calculated by Method 3 is plotted in Figure 9(a) to 9(c) for three steel temperatures. For saturated liquid fuel (at 3120 K) the only two heat sources are the latent heat and cooling down of solid fuel. However the proportion of heat lost from liquid fuel increases with increasing fuel temperature, and becomes the dominant source above about 3600 K.

The heat gained by the steel phases as a proportion of total heat transferred to the steel is plotted in Figure 9(d) to 9(f) for three fuel temperatures. There are three heat sinks: (a) heat up of solid steel, (b) latent heat absorbed by melting steel, and (c) heat up of the liquid steel layer. The heat absorbed by solid steel is dominant at low steel temperatures, but rapidly decreases for steel temperatures approaching the steel melting point. More heat is absorbed by steel melting than by the heating up of the molten steel layer.

The heat lost and gained by all phases predicted by the four methods for an initial fuel temperature of 3600 K and three steel temperatures are plotted in Figure 10(a) to 10(c). Method 3k predicts higher heat loss from liquid fuel due to the higher liquid fuel thermal conductivity. The fact that the heat sources and sinks add up to unity confirms that energy is being conserved, and the phase change constants are being correctly calculated by Meltit.

Transient quantities

All transient quantities obey the $\sqrt{t}$ law. The interface of the thermal front penetrating the liquid is not sharply defined, but a reasonable definition is $2\sqrt{\alpha_{1,l}t}$. The solidification front is $|X_1| = 2\lambda_1\sqrt{\alpha_{1,s}t}$. Both of these quantities are plotted in Figure 11(a) for various values of λ_1. When λ_1 is close to unity, which is the case for low temperature fuel and steel, the crust interface follows hard on the heels of the thermal front. The velocities of the thermal front and crust interface are $\sqrt{\alpha_{1,l}/t}$ and $\lambda_1\sqrt{\alpha_{1,s}/t}$ respectively, and are plotted in Figure 11(b). The velocities rapidly decrease to very small values even on a millisecond timescale.

The total heat transferred from fuel to steel is given by equations (2.11) and (2.26). It is plotted in Figure 11(c) for fuel initially at 3200 K and various initial steel temperatures.

Summary of the exact solution for perfect contact

The application of the transient heat conduction analysis to liquid UO_2 in perfect thermal contact with solid steel gives the following results.

- Fuel tries to freeze on contact with steel for all realistic fuel temperatures. Steel may or may not melt at the interface, depending on the initial temperatures of the contacting materials, as shown in Figure 5.

- The assumption that constant materials properties can be assigned to the four phases is only approximately valid for UO_2/steel. This is demonstrated by the spread in results shown in Figure 5. It is necessary to take into account the temperature-variation of steel properties, and to evaluate properties at a suitable reference temperature. Calculations are least accurate when the steel properties are evaluated at the initial (bulk) steel temperature.

- The most up-to-date prediction of the conditions for melting of steel structure surface in contact with liquid UO_2 by the heat conduction method is Method 3 of Figure 5. The most up-to-date estimate of the fuel solidification constant and fuel-steel interface temperatures are given by Figures 6(a) and 7(a) respectively. The time-dependent crust growth can be deduced by reference to Figure 11(a).

5.3 Results using the approximate solutions

Two approximate solutions to the heat conduction equation - the Amateur Mathematician and the Naive Physicist - are described in Section 3. The results obtained using these approximate solutions are compared in this subsection against results from the exact solution. The results have been calculated using material properties evaluated by Method 1, since this Method does not require iteration to find the mid-point temperatures of the phases.

The phase change map

The criteria of No Fuel Freezing and No Steel Melting are plotted in Figure 12. The approximate solutions are both very close to the exact solution. In particular the three solutions are much closer than the spread associated with varying materials properties (see Figure 5). There is no significant difference between the two approximate solutions.

The phase change constants

The fuel solidification constants for a range of fuel temperatures and four steel temperatures are plotted in Figures 13(a) and 13(b). The solidification constant is underestimated by both approximate solutions at fuel temperatures close to the melting point, but more so (by up to 15 %) by the Naive Physicist. The differences are more pronounced for low steel temperatures.

The steel melting constants are shown in Figure 13(c). The approximate solutions calculate the melting constant using a single value for the solidification constant, so the melting constants calculated by the approximate solutions are a function of

steel temperature only. Nevertheless both solutions calculate the steel lambda as well as can be expected.

Fuel-steel interface temperature

The fuel-steel interface temperatures according to all three solutions are plotted in Figures 14(a) to 14(c) for a range of steel temperatures and three fuel temperatures. It can be seen from Figure 14 that both approximate solutions give a good estimate of the interface temperature, to within about 60 K over a wide range of fuel and steel temperatures. Note that for the approximate solutions there is a discontinuity in interface temperature at the steel melting temperature.

Heat losses and gains

The heat lost and gained by the various phases is not plotted, but examination of printed output shows that the Naive Physicist approach conserves energy for the fuel phases, but not for the steel phases. This is because the steel melting constant is computed using an estimate for the fuel solidification constant, rather than the true value of the solidification constant. Energy conservation can be achieved only if iterations are allowed to solve for the phase change constants simultaneously. Nevertheless the error in energy conservation is small, especially for the range of temperatures of interest, and the relative proportions of energy change are very close to the exact solution.

The Amateur Mathematician approach also does not conserve energy for steel, for the same reason as the Naive Physicist approach. In addition the proportion of energy transferred from each phase is calculated using slightly different expressions from those used to formulate the energy equations, so that energy conservation in the fuel is not exact either.

Summary of approximate methods

The two approximate solutions - the Amateur Mathematician and the Naive Physicist - effectively simplify the energy equations as quadratic functions of the fuel and steel phase change constants, which can be solved directly without iteration. Although neither approach conserves energy exactly, key results are reproduced rather well in comparison with the exact solution for a wide range of fuel and steel temperatures.

The success of the Naive Physicist approach indicates that transient fuel crust growth can be reproduced satisfactorily by a model which assumes point temperatures in the fuel and steel phases. This assumption is essentially used in SIMMER-III, which suggests that SIMMER-III should calculate crust growth correctly even for highly transient conditions.

5.4 Results for a transient gap conductance

The formulation for the case of an ideal transient gap conductance, h_g, is described in Section 4. Results using seven values of h_g have been computed using Meltit. The seven values are listed in Table 1, and span the range of the thermal conductances in the four phases, $\omega_{1,l}$ etc, which have the same units as h_g. Two types of results are presented: (a) the influence of gap conductance on the phase change temperature map, and (b) the effect of gap conductance on interface temperatures, transient heat flux and transient crust growth for one pair of fuel and steel temperatures (3600 K/1200 K respectively). All material properties are evaluated using Method 1 described in Section 5.1, but the material properties used to generate the results shown in Figures 15 to 17 differ slightly from the values described in Appendix B.

Effect of gap conductance on the phase change temperature map

The effect of a gap conductance on the phase change temperature map is illustrated in Figures 15 and 16. When there is no thermal resistance, i.e. $h_g = \infty$, the phase change map is the same as that described in Section 5.2 (see Figure 15(a)). When the value of h_g becomes comparable to the thermal resistance of the most conductive phase, which is solid steel, the range of temperatures for which simultaneous fuel freezing and steel melting occurs becomes narrower, but the shape of the map does not alter substantially (see Figure 15(b)). However the effect of reducing the value h_g further, so that it is comparable with the solid fuel and liquid steel thermal conductances, is to create a region in which neither fuel freezing nor steel melting occurs (see Figure 15(c) and 15(d)).

The phase change maps in Figure 16 depict even lower values of gap conductance, and are plotted with the fuel temperature axis on a smaller scale, than the maps in Figure 15. Very low values of gap conductance increasingly restrict the range of temperatures for which fuel freezing and steel melting can occur.

Effect of gap conductance on heat fluxes and crust growth

The variation of some key quantities with gap conductance is listed in Table 1, and illustrated in Figure 17 for a single pair of fuel/steel initial temperatures (3600 K/1200 K respectively). For this pair of temperatures, simultaneous fuel freezing and steel melting occur for perfect thermal contact, only fuel freezing occurs for "moderate" values of gap conductance, whilst no phase changes at all are predicted for a very low gap conductance. The heat fluxes from fuel to steel need to be reduced only to 80 % of the values calculated for perfect thermal contact for the steel not to melt, whilst a reduction to about 20 % of the perfect value is sufficient to prevent any phase change. The value of the gap conductance clearly has a major influence on the rate, and the occurrence, of fuel crust growth on steel.

5.5 Comparison with experimental results for steel structure melting

Experiments involving UO_2-based melts do not generally measure the interface temperature between liquid UO_2 and steel. The only clear-cut results are from experiments which demonstrate, using post-test examination, that steel melting did not occur. In this case the interface temperature cannot have exceeded the steel melting point in the test. If steel melting is detected by post-test examination it is usually not clear whether melting was initiated instantaneously on initial melt-structure contact, or whether it occurred later. For example a fuel crust might initially form on a steel wall, but if the timescale of the experiment is sufficiently long, the crust can be eroded and the heated steel ablated by the melt flow. In general more suitable results are obtained from experiments in which the heat capacity of the steel structure is large since this reduces the possibility of bulk steel melting later in the test. Tests performed using thick-walled tubes and plates satisfy this condition; tests involving pin bundles generally do not.

A selection of suitable experiments which involve molten UO_2, or a UO_2-based melt mixture, coming into contact with steel structures are compiled in Table 1 of ref. [6]. The experiments include melts which used a UO_2/Mo thermite mixture, though it is likely that the thermite mixture has a higher thermal conductivity than UO_2 due to the presence of metallic Mo. The tests mainly involve melt penetration in circular or rectangular steel-walled channels. The initial melt and steel temperatures listed in Table 1 of ref. [6] are plotted in Figure 18. The tests in which steel melting is considered to have occurred on melt-structure contact are distinguished in the figure by having their symbols circled. For experiments performed at relatively low initial structure temperatures, steel melting was not detected. At higher structure and fuel temperatures steel melting on fuel-structure contact is thought to have occurred.

Steel melting criteria according to the heat conduction analysis for perfect melt-structure contact are also plotted in Figure 18. The original calculation by Epstein predicts melting for several tests in which no melting was detected, but this is mainly because the temperature-dependence of the solid steel physical properties are not taken into account. The criteria for steel melting using Methods 3 and 3k differ in the value of the thermal conductivity assumed for the melt (2.5 and 5.6 W/m/K respectively - see Section 5.1). Both of these criteria predict steel melting for initial structure temperatures above about 1100 to 1200 K. Figure 18 shows that the criteria agree with experimental data with the following exceptions:

- Some ANL tube tests, using thermite, recorded steel melting for relatively low initial structure temperatures. However these tests were performed for sufficiently long times that crust growth and erosion *might* have occurred [7]. In other words, the steel melting might not have occurred on initial contact but later on, after the crust had been eroded. Nevertheless the test results do indicate a tendency towards more pronounced steel melting as the steel initial temperature increases.

- Some TRAN tests indicate steel melting for lower steel temperatures than predicted. However the steel melting detected in the test with steel wall temperature at 873 K appears to have occurred only near the channel entrance. A particular feature of the TRAN tests was the relatively high UO_2 velocities in the tubes (~ 10 m/s) [8]. In addition it is reported that the degree of steel melting seems to have been influenced by the driving pressure. Moreover the test series indicates steel melting fairly close to the steel melting criteria, given the uncertainties in physical properties.

- Two Geyser tests - tests 7 and 8 - did not detect steel melting despite an elevated wall temperature of 1000 °C along a 30 cm inlet portion of the steel tubes. Steel melting is predicted by the criteria, but no steel melting was detected.

In summary, the experimental data for steel structure melting is approximately compatible with the criteria predicted by heat conduction. However there are some notable inconsistencies, in particular the absence of steel melting in Geyser tests 7 and 8.

6. CONCLUSIONS

The transient heat conduction equations for the case of initially liquid UO_2 making thermal contact with solid steel have been solved using a computer code. In particular fuel-steel interface temperatures, a criterion for steel structure melting and the fuel solidification constant have been evaluated using the most up-to-date materials properties. As well as obtaining an exact solution, approximate solutions have been derived and the effect of a gap conductance has been investigated.

The criterion for steel melting predicted by the heat conduction equations for perfect thermal contact has been compared with available experimental data. Although the criterion seems to approximately estimate the rubicon which separates non-melting from melting structure, there are some contradictory test results which indicate that the method is not entirely correct.

The computer program used to solve the transient heat conduction equations is available on IBM workstations so that calculations can be quickly repeated using alternative materials properties.

7. REFERENCES

[1] M. Epstein, "Heat conduction in the UO_2-cladding composite body with simultaneous solidification and melting", Nucl. Sci. Eng., vol. 51, p. 84 (1973).

[2] N. K. Hayden, "An analytic model of freezing liquid penetration in tube flow", Trans. ASME, p. 671 (1981).

[3] K. Morita, E.A.Fischer and K.Thurnay, "Thermodynamic properties and equations of state for fast reactor safety analysis, Part II: Properties of fast reactor materials", Nucl. Eng. Des., in press (1998).

[4] G. Berthoud, "Relocation of molten fuel: determination of the interfacial resistance", Proc. IAEA/IWGFR Technical Committee on Material-Coolant Interactions and Material Movement and Relocation in LMFRs, O-arai (1994).

[5] M. Epstein et al, "Analytical and experimental studies of transient fuel freezing", Proc. Fast Reactor Safety and Related Physics Mtg, Chicago (1976).

[6] D. A. McArthur et al, "The TRAN experiment series in the Sandia ACRR facility", Proc. LMFBR Safety Topical Meeting, Lyon (July 1982).

Table 1: Influence of gap conductance on heat transfer and crust growth

* Fuel & steel temperatures (K): 3600.0 1200.0
* Fuel & steel lambdas w/o a gap: .74302 .09189

* Thermal resistances in the 4 phases:
w1l = dsqrt(rho1l*cp1l*con1l): 2545.4
w1s = dsqrt(rho1s*cp1s*con1s): 4756.7
w2l = dsqrt(rho2l*cp2l*con2l): 8372.9
w2s = dsqrt(rho2s*cp2s*con2s): 13492.5

Quantity	hg (W/m2/K.s**.5): NO GAP	50000.	12500.	6500.	4000.	2000.	1000.	500.
ichph	-	4	3	3	3	3	3	1
hramfu	.7430	.7157	.6400	.5605	.4731	.3025	.1032	.0000
htin1	1840.0	1955.1	2229.1	2456.9	2652.3	2912.3	3077.4	3217.8
htin2	1840.0	1794.2	1694.9	1608.7	1532.1	1421.1	1329.5	1272.1
hqtot	1.0	.9336	.7747	.6397	.5198	.3460	.2028	.1129
hqlqfu	.25017	.2633	.3019	.3464	.4007	.5294	.7664	1.0000
hqltfu	.32559	.3359	.3620	.3840	.3988	.3831	.2230	.0000
hqslfu	.42425	.4008	.3361	.2696	.2005	.0875	.0106	.0000

KEY
---
ichph: Flag to define which phase changes are occurring at the interface -
1: No fuel freezing; no steel melting
2: No fuel freezing; steel melting
3: Fuel freezing; no steel melting
4: Fuel freezing and steel melting
hramfu: Fuel lambda
htin1: Fuel-side interface temperature
htin2: Steel-side interface temperature
hqtot: Heat flux as a proportion of the heat flux with no gap
hqlqfu: Heat lost from liquid fuel as a proportion of total heat transfer
hqltfu: Latent heat loss as a proportion of total heat transfer
hqslfu: Heat lost from solid fuel as a proportion of total heat transfer

Table 2: Contact mode and conditions in experiments which have investigated the freezing of UO_2-dominant melts

Experiments	Contact mode	Melt type/ temp (K)	Steel temp (K)	Conditions
ANL Channel [T1]	Circular channel	UO_2/Mo 3473	300, 573, 673, 773, 873, 1173	Melt injected in thick-walled steel tubes, inner diameters between 3 and 10 mm.
ANL Spencer's Bundle tests [T2]	7-pin and 37-pin bundles	UO_2 /Mo 3473	573, 873, 973, 1173	0.37 mm thick steel cladding on test pins. 0.5 Kg or 2 Kg melt injected axially.
Sandia TRAN Series I [T3]	Tube	3200, 3600, 3700, 3750, 3750,3570	673, 773, 873, 943, 2*1173	Molten UO_2 injected into a 3.2 mm inner diameter thick-walled steel tube.
ANL SHOTGUN tests [T4]	Tube	UO_2/Mo 3470 K	293 K	Melt injected downwards into thick-walled steel tubes of 6.35 mm ID
ANL Jet [T5]	Jet	UO_2/metal mp+120K	300 400	UO_2/metal mixture impinging a horizontal steel plate.
Cadarache BF1 [T6]	Molten pool	UO_2 > 3120	(~700 K)	UO_2 melted inside a steel crucible, cooled by external flow of sodium.
ISPRA BLOKKER I [T8]	Jet	UO_2 3300	360 700	Molten UO_2 jet impinging thick stainless steel plates at various angles.
ISPRA BLOKKER II [T8]	Channel: circular & rectangular	UO_2 3300	700	Stainless steel channels with hydraulic diameters: 4.0, 8.5, 9.9 mm.
Winfrith SMPR [T7]	Tube	3600	293	Melt injected at ~ 3 m/s into 3.3 mm ID steel-walled tubes.
Grenoble Geyser [T7,T8]	Tube	UO_2 3273	293 1273	Molten UO_2 injected into 4 mm ID steel tubes. Walls in 2 tests elevated to 1273 K at the inlet.

References

[T1] EPSTEIN et al, "Analytical and experimental studies of transient fuel freezing", Fast Reactor Safety Mtg, Chicago, 1976.
[T2] SPENCER et al, "Summary and evaluation of reactor-material fuel freezing tests", Intl mtg on FR Safety Technology, Seattle, 1979.
[T3] GAUNTT et al, "Analysis of the TRAN in-pile fuel freezing experiments", FR Safety mtg, Knoxville, 1985.
[T4] SPENCER et al, "Results of recent reactor-material tests on dispersal of oxide fuel from a disrupted core", FR Safety mtg, Knoxville, 1985.
[T5] SIENICKI et al, "Analysis of reactor material experiments investigating oxide fuel crust stability .. in jet impingement", FR Safety mtg, Knoxville, 1985.
[T6] CAMOUS et al, "SCARABEE - single and 2-phase natural convection in sodium and molten core materials", Sci. Tech. FR safety, Guernsey, 1986.
[T7] M. Schwarz et al, "Interpretation of out-of-pile expts on the propagation and freezing of molten fuel", 13th LMBWG Mtg, UKAEA Winfrith, 1988.
[T8] LE RIGOLEUR et al, "Review of European out-of-pile tests ....", IWGFR/IAEA/89 Material Coolant Interactions Mtg, O-arai, 1994.

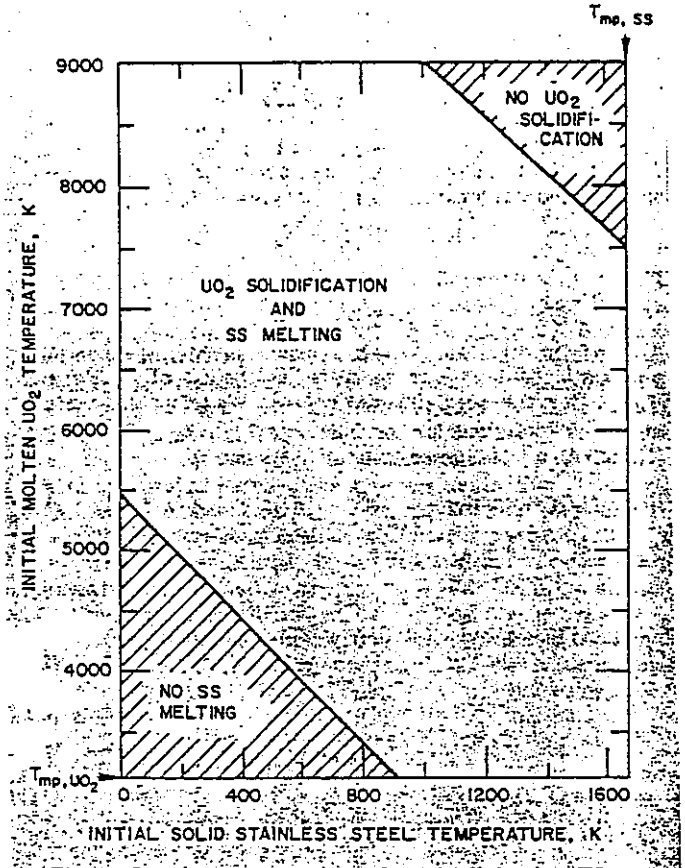

Fig. 2. Initial-temperature map for initially molten UO_2 contacting initially solid stainless steel, showing the region (unshaded) in which simultaneous UO_2 solidification and steel melting occur.

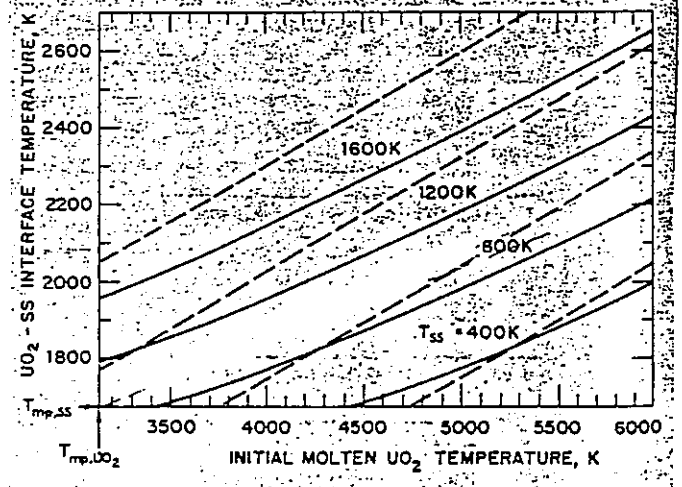

Fig. 3. UO_2-SS interface temperature as a function of initial molten UO_2 temperature; initial solid stainless-steel temperature as parameter. Dashed line indicates behavior that is obtained when phase change effects are ignored.

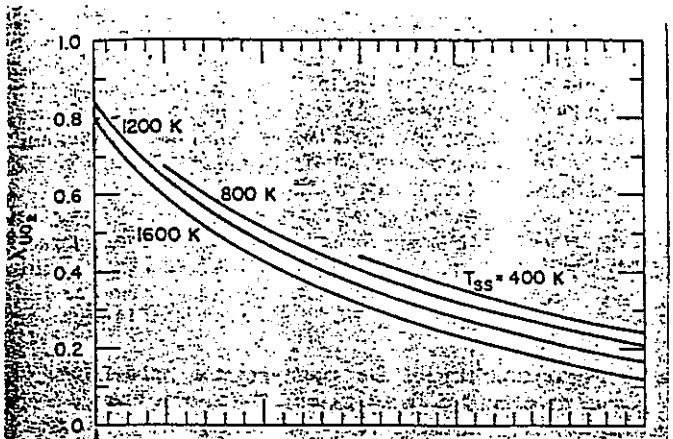

Fig. 4. UO_2 solidification constant as a function of initial molten UO_2 temperature; initial solid stainless-steel temperature as parameter.

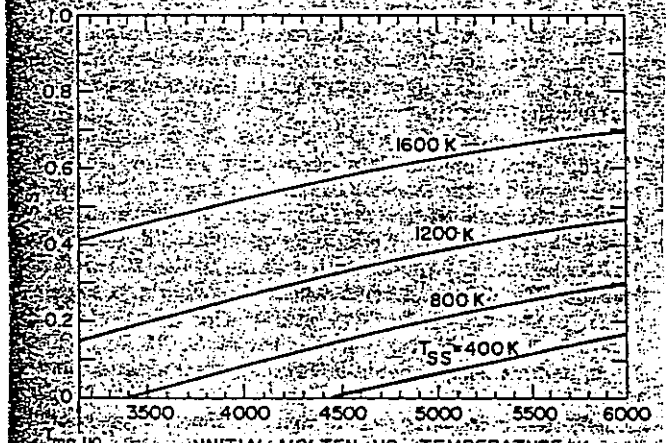

Fig. 5. Stainless-steel melting constant as a function of initial molten UO_2 temperature; initial solid stainless-steel temperature as parameter.

Fig. 1: Results and predictions originally calculated by Epstein (1973)

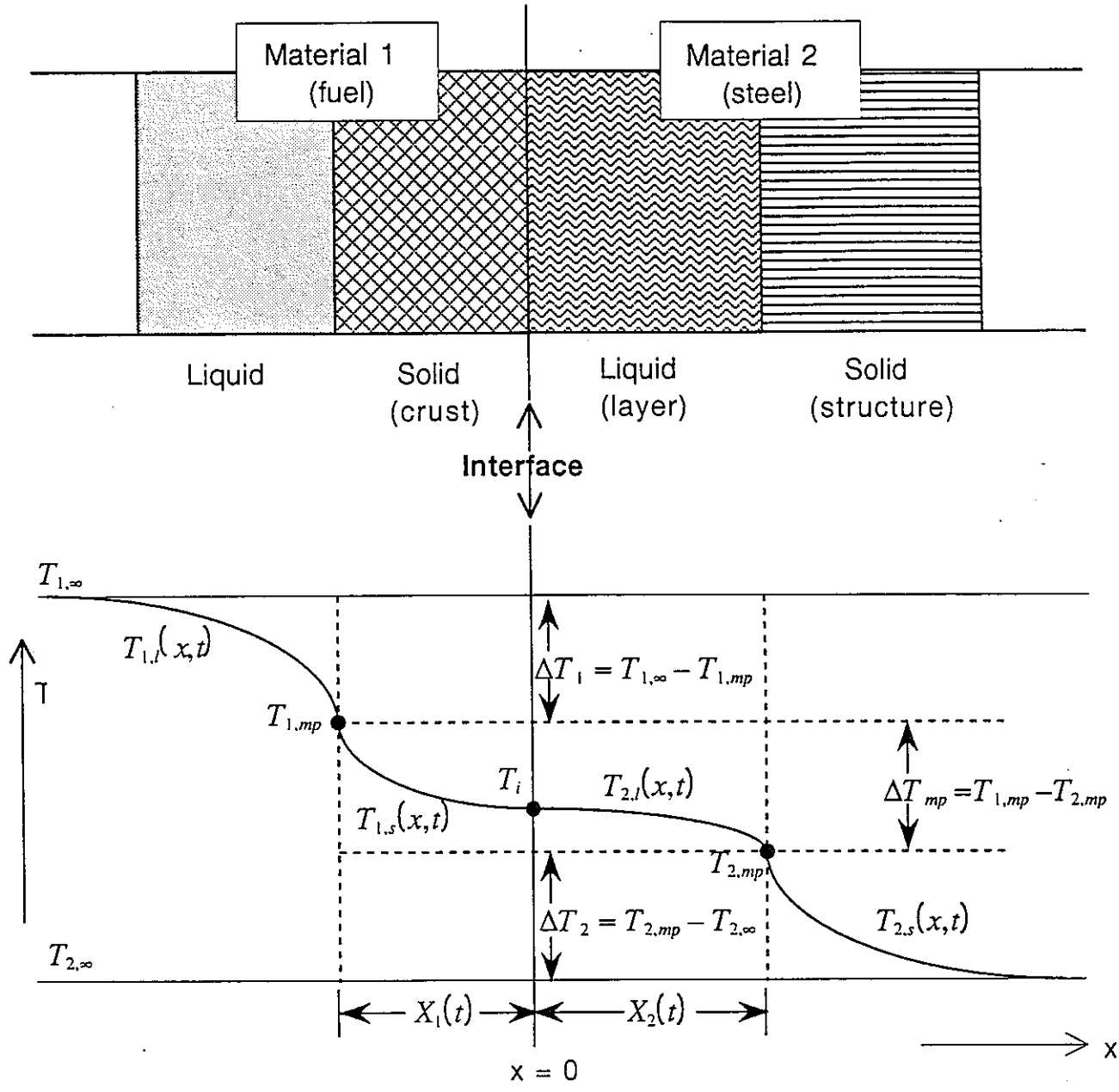

Fig.2: Schematic representation of the configuration and temperature profiles during simultaneous liquid freezing and solid melting

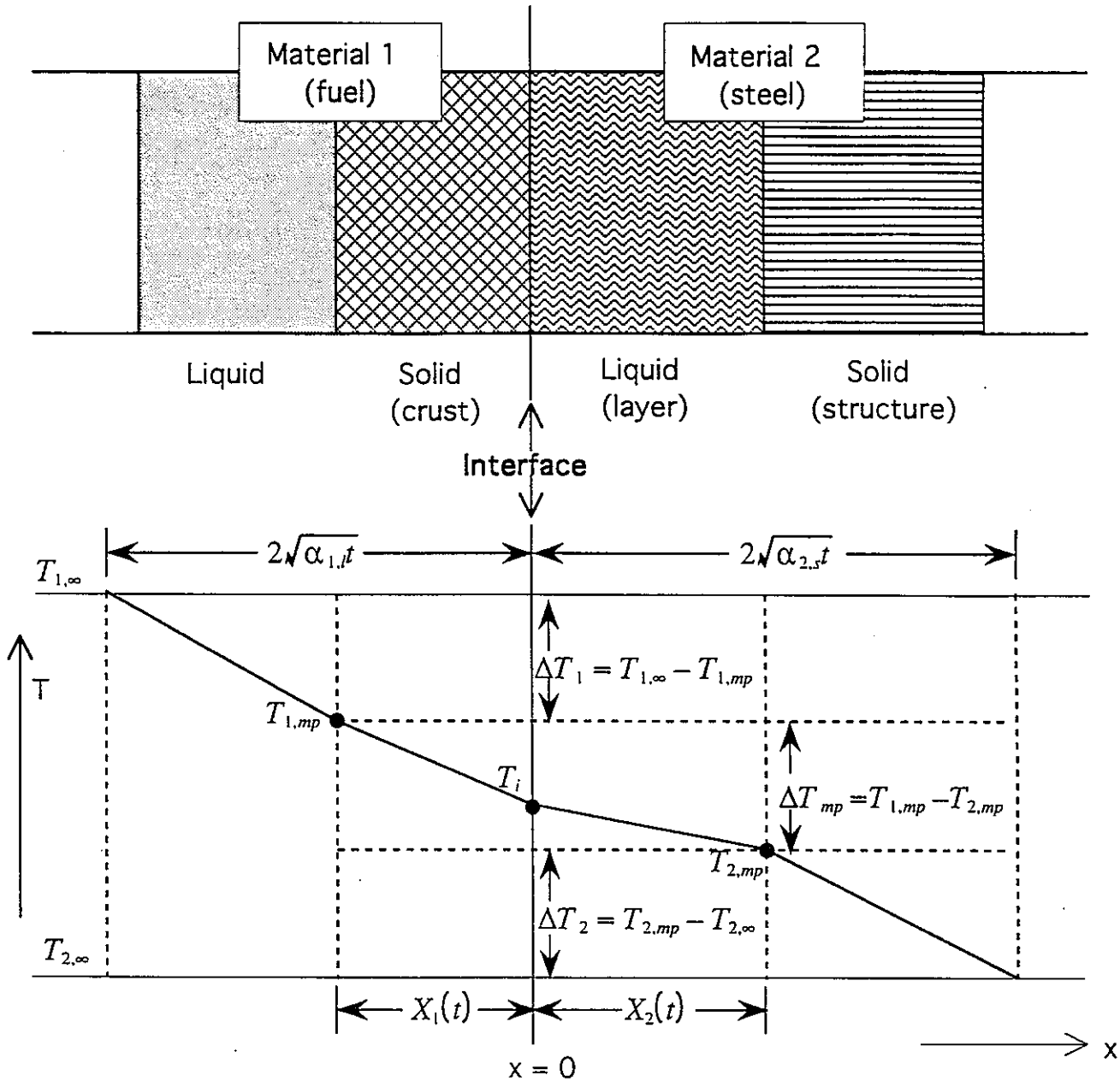

Liquid fuel

$$\bar{T}_{1,l} = \frac{1}{2}\left[T_{1,\infty} + T_{1,mp} \right]$$

Liquid steel

$$\bar{T}_{2,l} = \frac{1}{2}\left[T_i + T_{2,mp} \right]$$

Solid fuel

$$\bar{T}_{1,s} = \frac{1}{2}\left[T_{1,mp} + T_i \right]$$

Solid steel

$$\bar{T}_{2,s} = \frac{1}{2}\left[T_{2,mp} + T_{2,\infty} \right]$$

Fig.3 : Temperatures profiles in the Naive Physicist approach

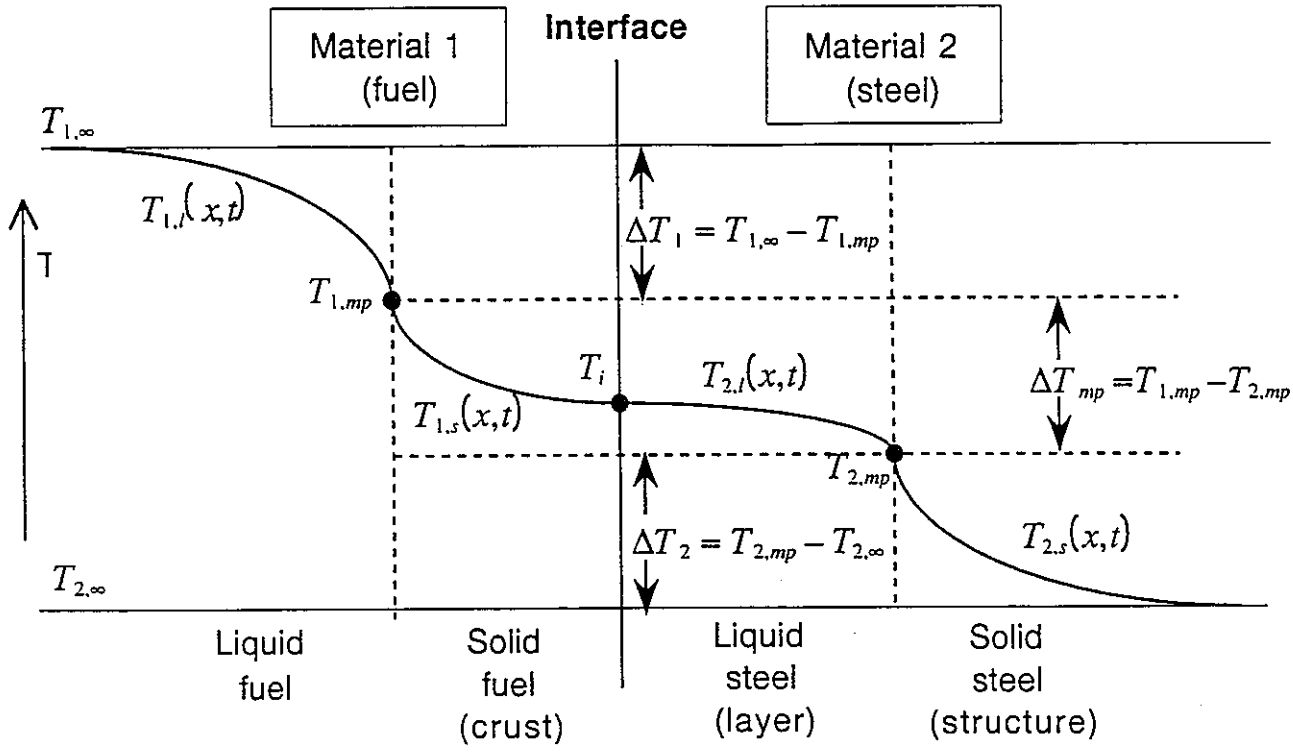

Method	Liquid fuel	Solid fuel	Liquid steel	Solid steel
M1	$\bar{T}_{1,l} = T_{1,mp}$	$\bar{T}_{1,s} = T_{1,mp}$	$\bar{T}_{2,l} = T_{2,mp}$	$\bar{T}_{2,s} = T_{2,mp}$
M2	$\bar{T}_{1,l} = T_{1,\infty}$	$\bar{T}_{1,s} = T_{1,mp}$	$\bar{T}_{2,l} = T_{2,mp}$	$\bar{T}_{2,s} = T_{2,\infty}$
M3	$\bar{T}_{1,l} = \frac{1}{2}[T_{1,\infty}+T_{1,mp}]$	$\bar{T}_{1,s} = \frac{1}{2}[T_{1,mp}+T_i]$	$\bar{T}_{2,l} = \frac{1}{2}[T_i+T_{2,mp}]$	$\bar{T}_{2,s} = \frac{1}{2}[T_{2,mp}+T_{2,\infty}]$

Fig.4 : Methods used to calculate the temperatures at which the properties of the phases are determined

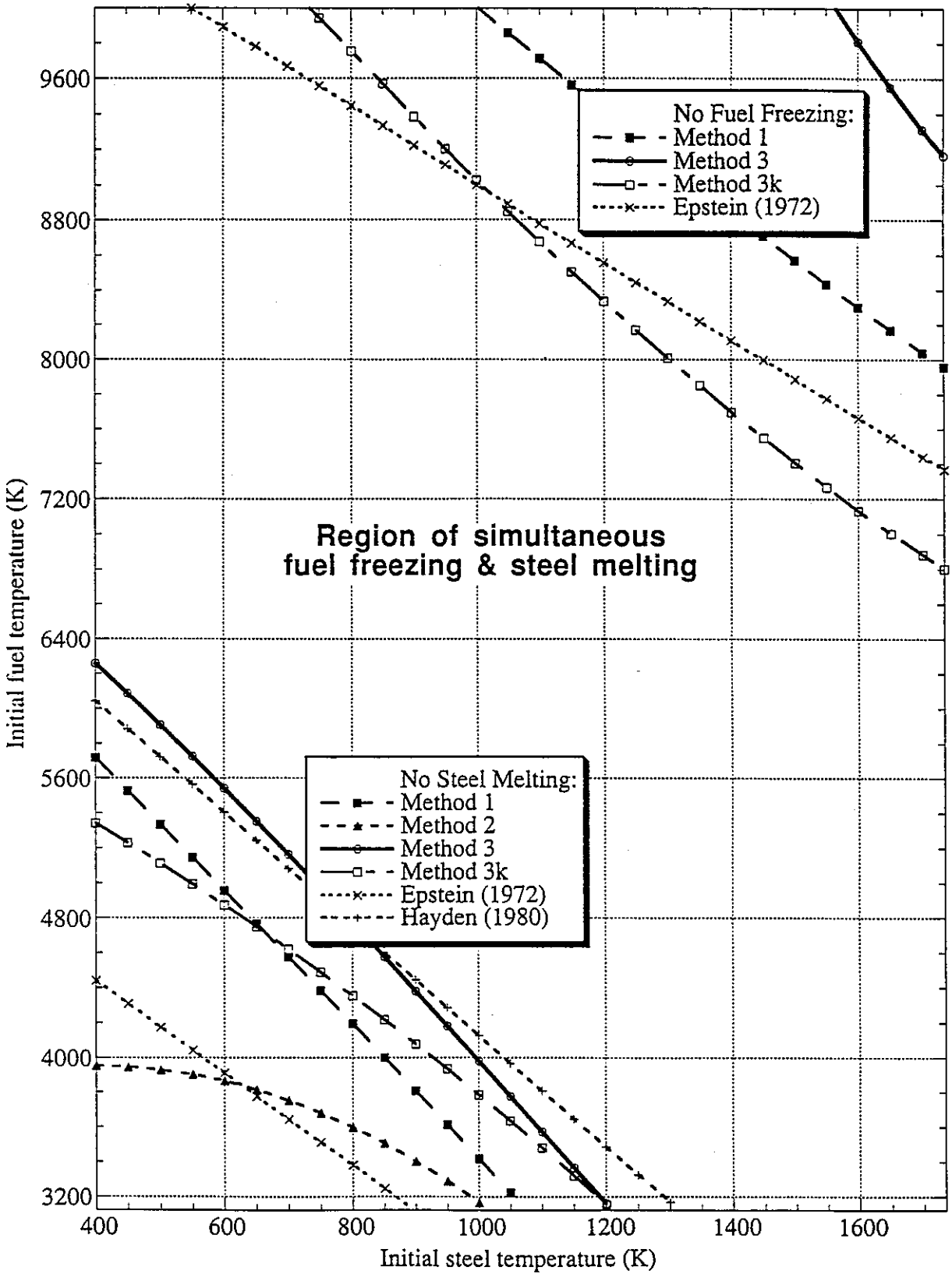

Fig. 5: The temperature map showing the boundaries of fuel freezing and structure melting by various Methods

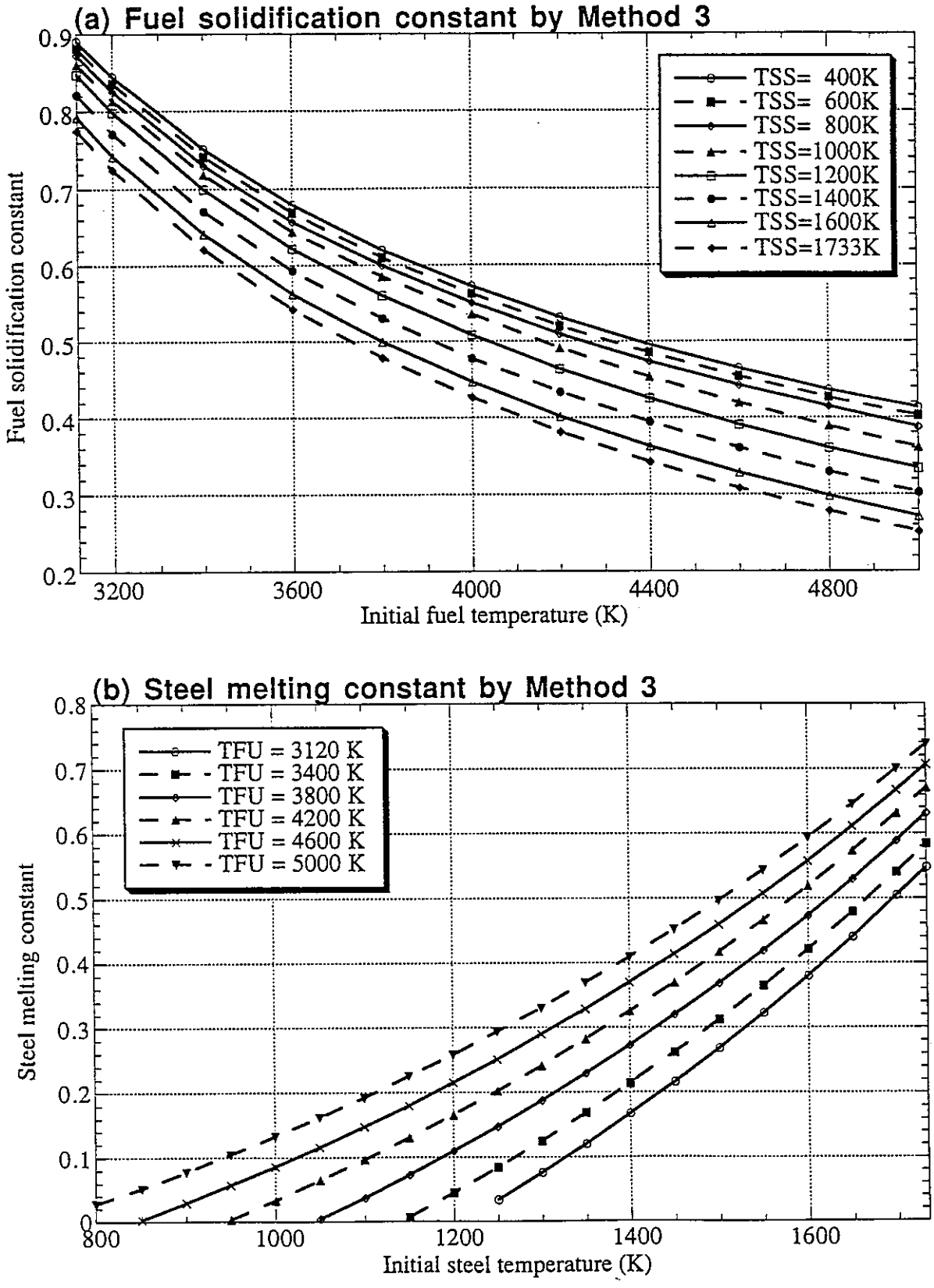

Fig. 6: The phase change "constants" using Method 3

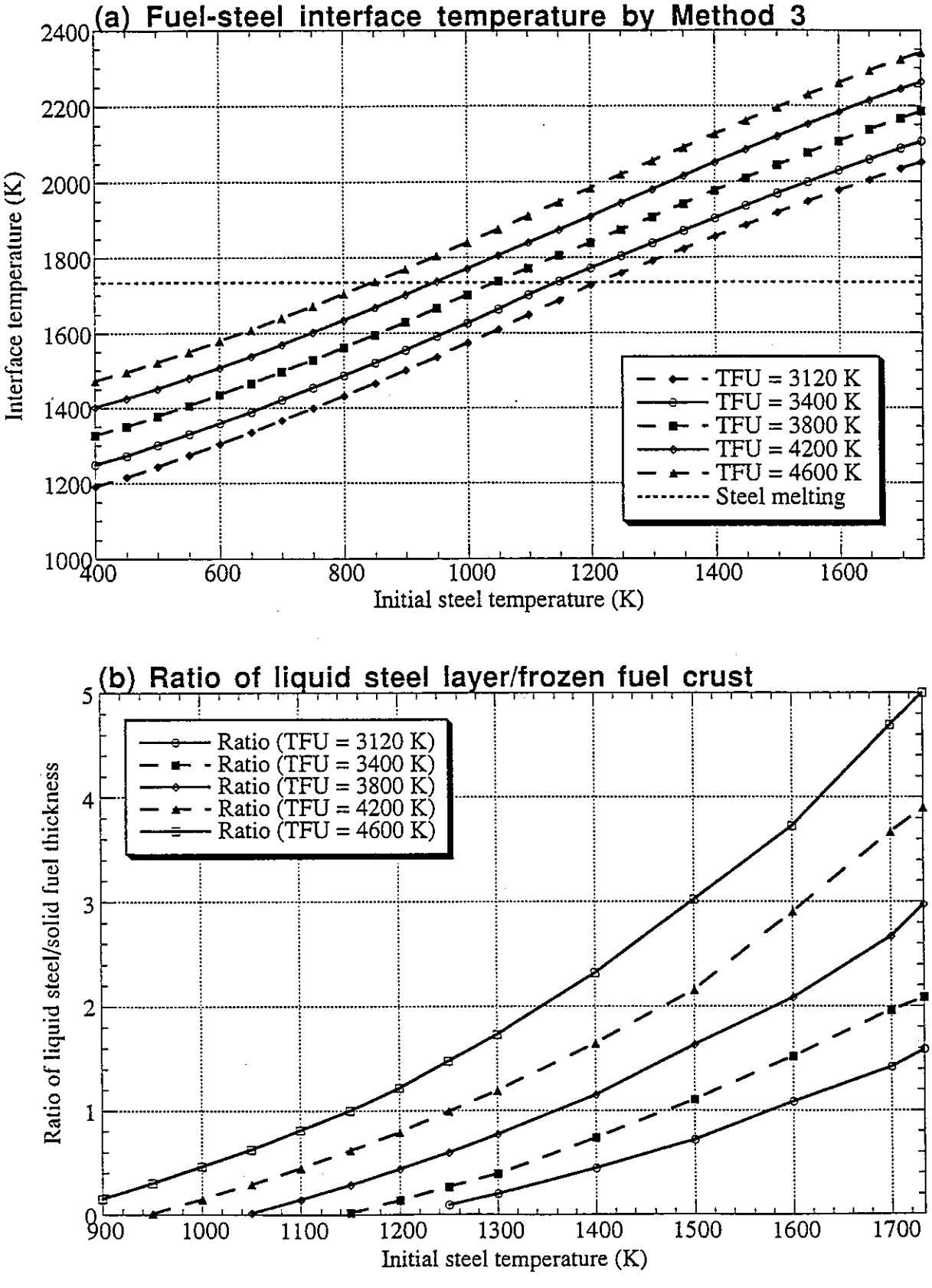

Fig. 7: The Fuel-Steel interface temperature and ratio of the liquid steel to the crust thickness using Method 3

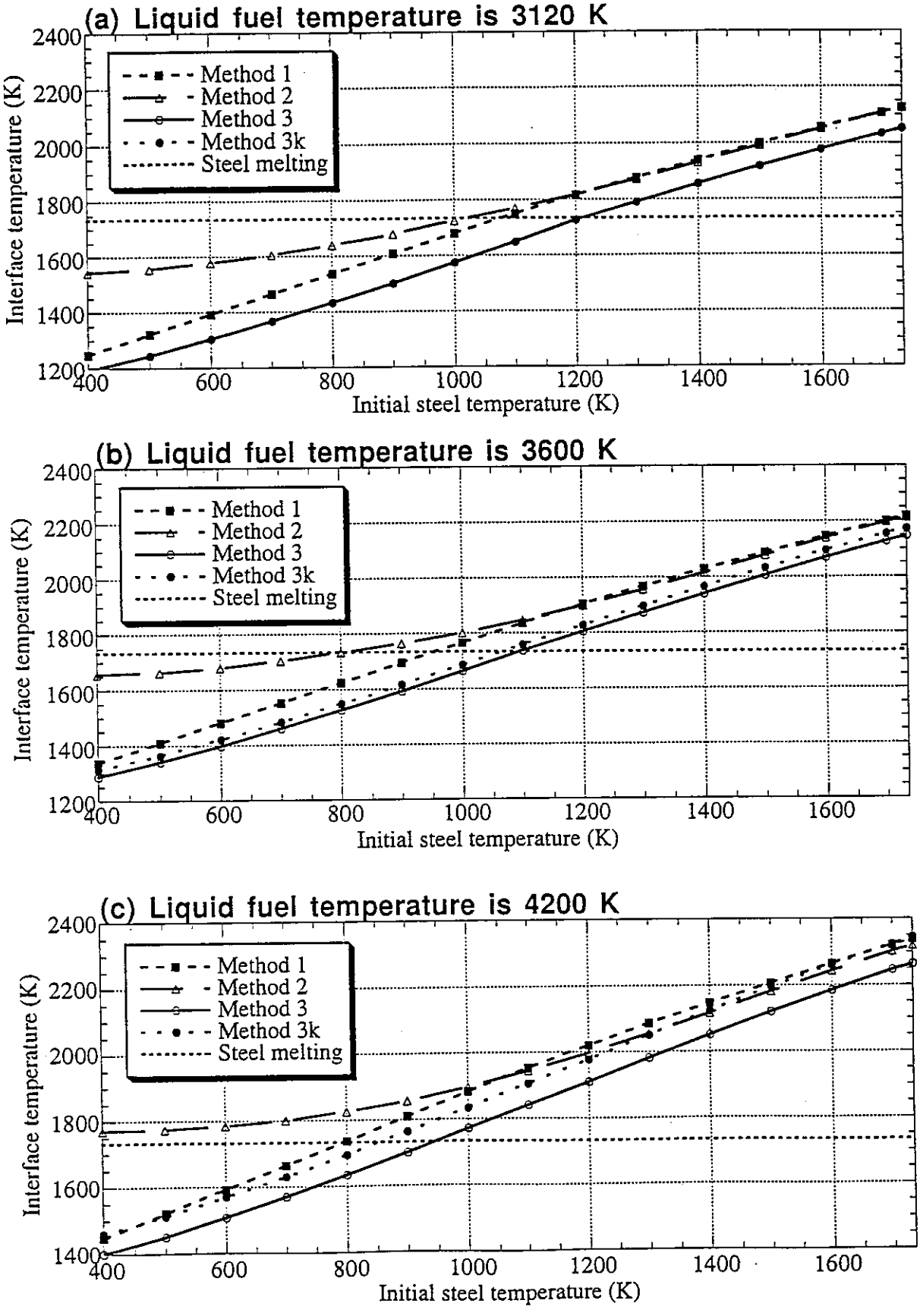

Fig. 8: The Fuel-Steel interface temperature using various Methods

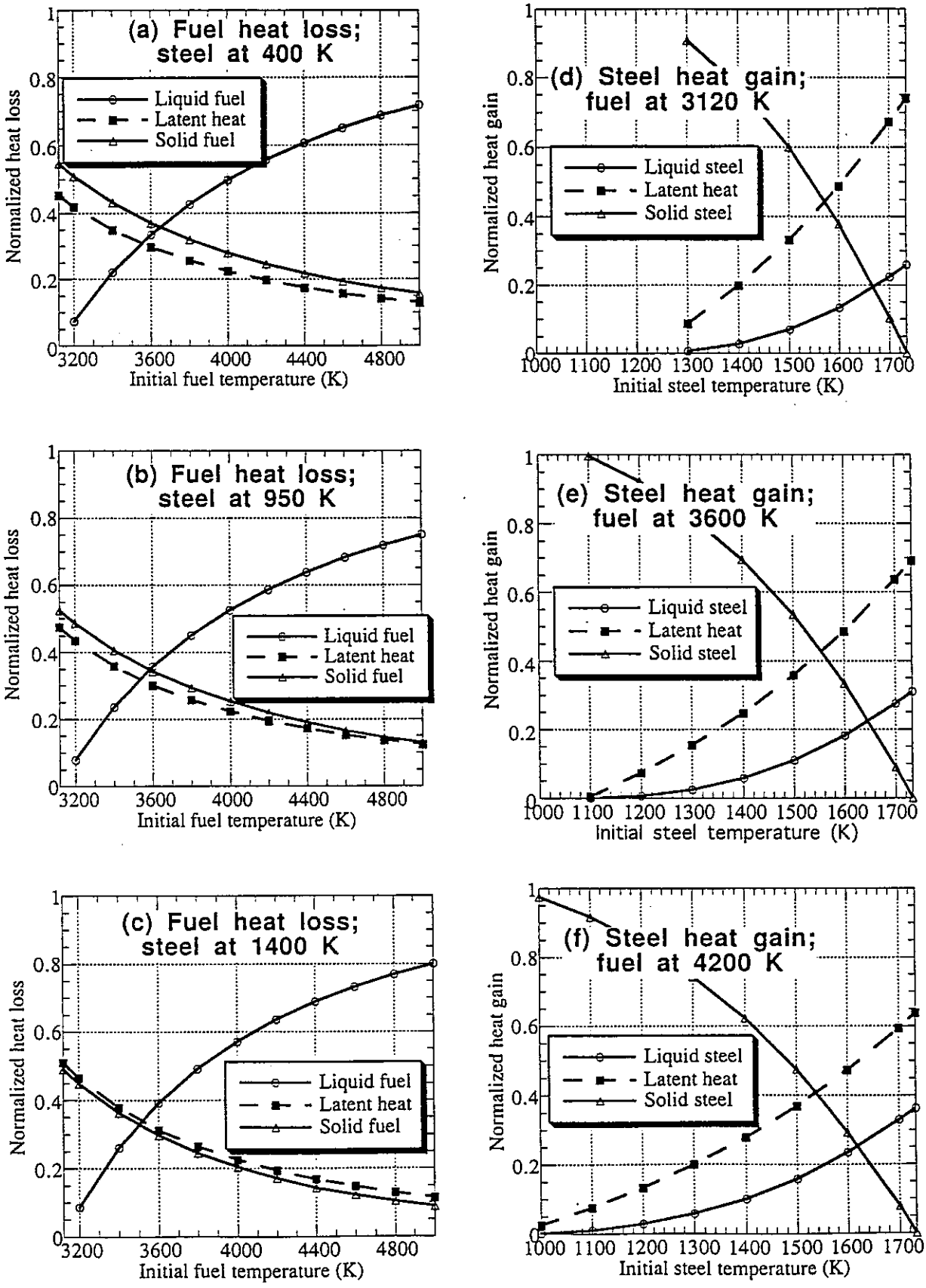

Fig. 9: Relative contributions to fuel-steel heat transfer from the fuel (left) and the structure (right)

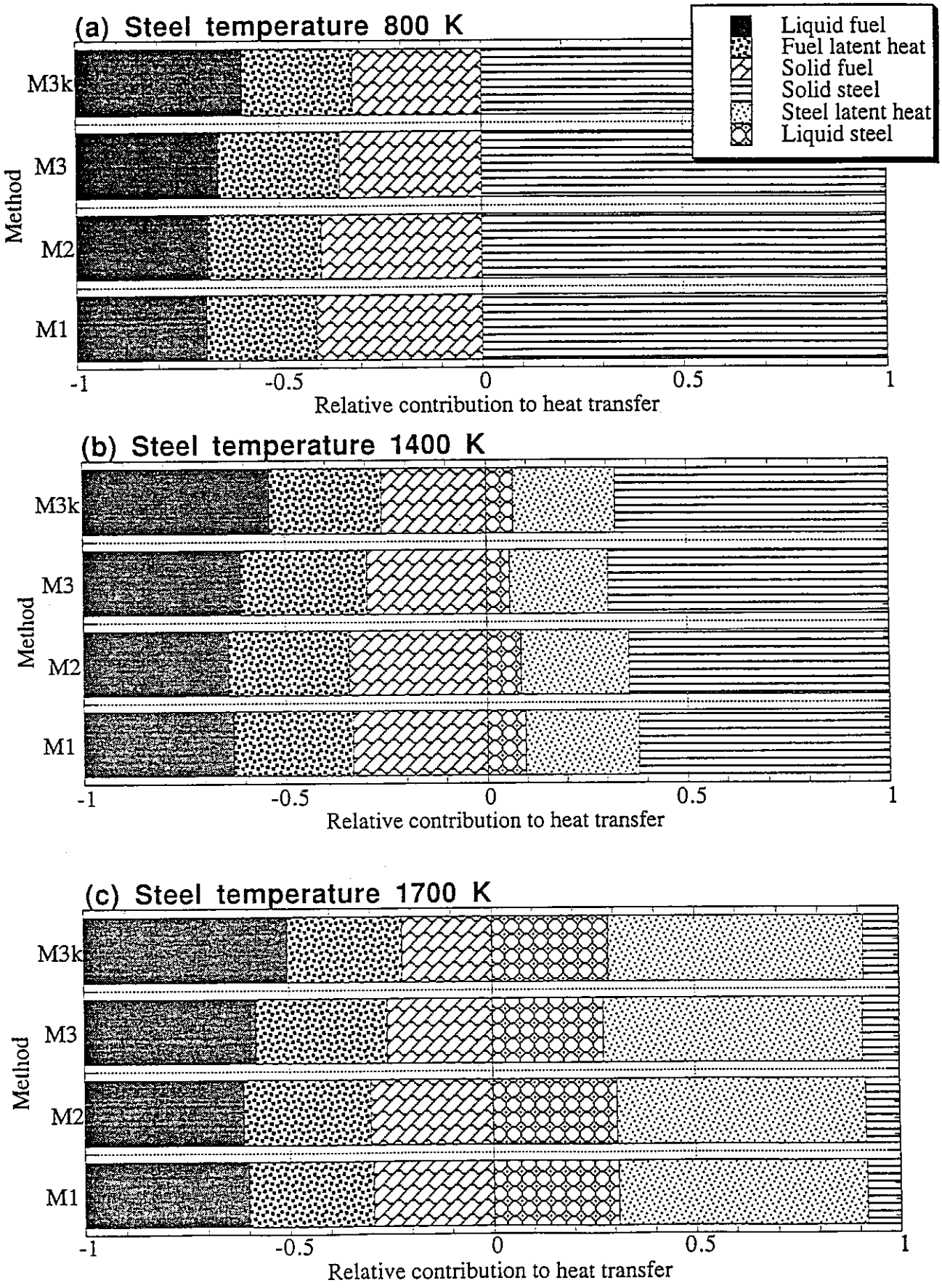

Fig. 10: Relative contributions to fuel-steel heat transfer for fuel initially at 3600 K

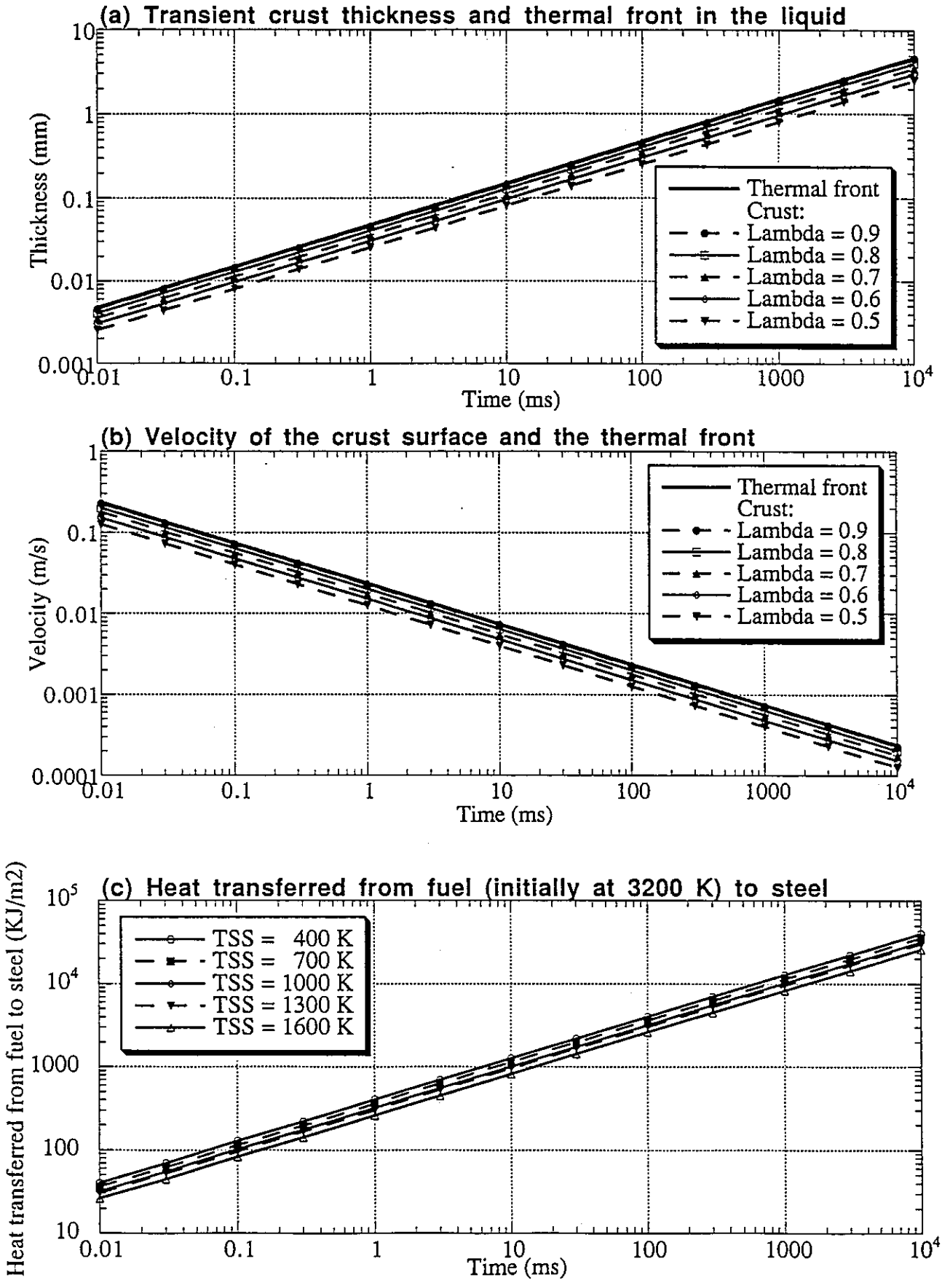

Fig. 11: Transient crust growth, penetration of the thermal front in the liquid fuel, and heat transfer from fuel to steel

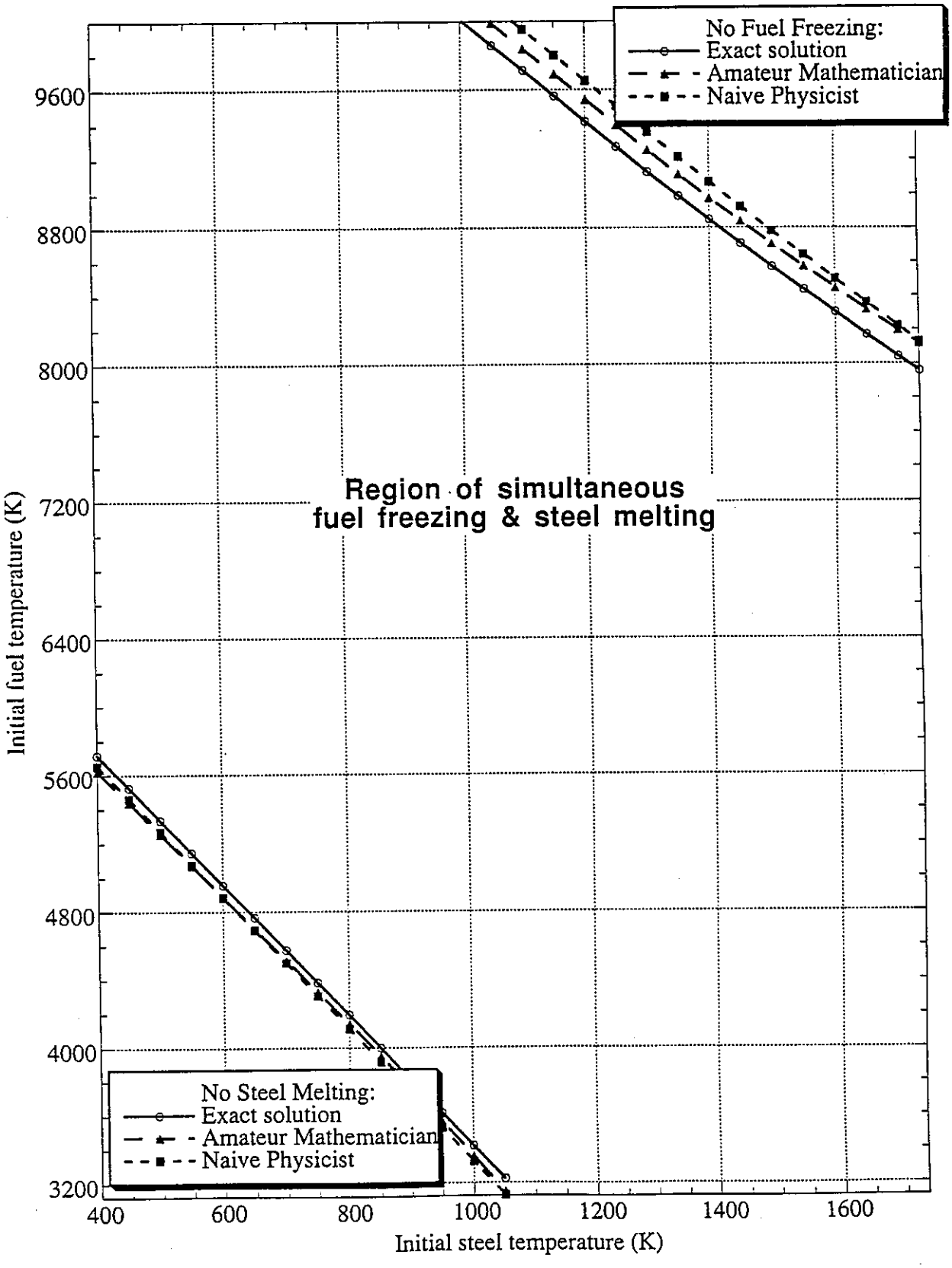

Fig. 12: The temperature map showing the boundaries of fuel freezing and structure melting according to exact and approximate solutions

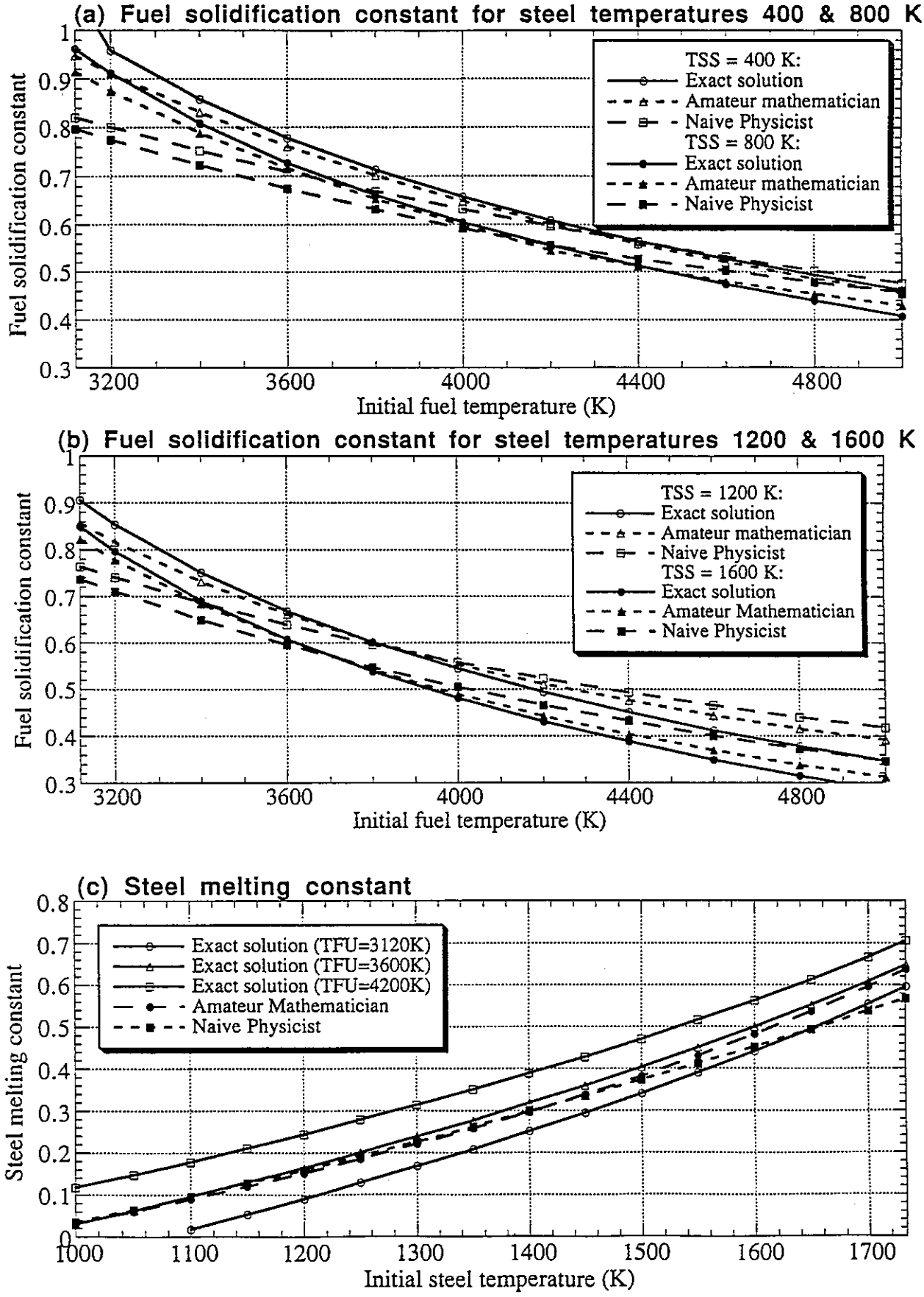

Fig. 13: The phase change "constants" using the exact and approximate solutions

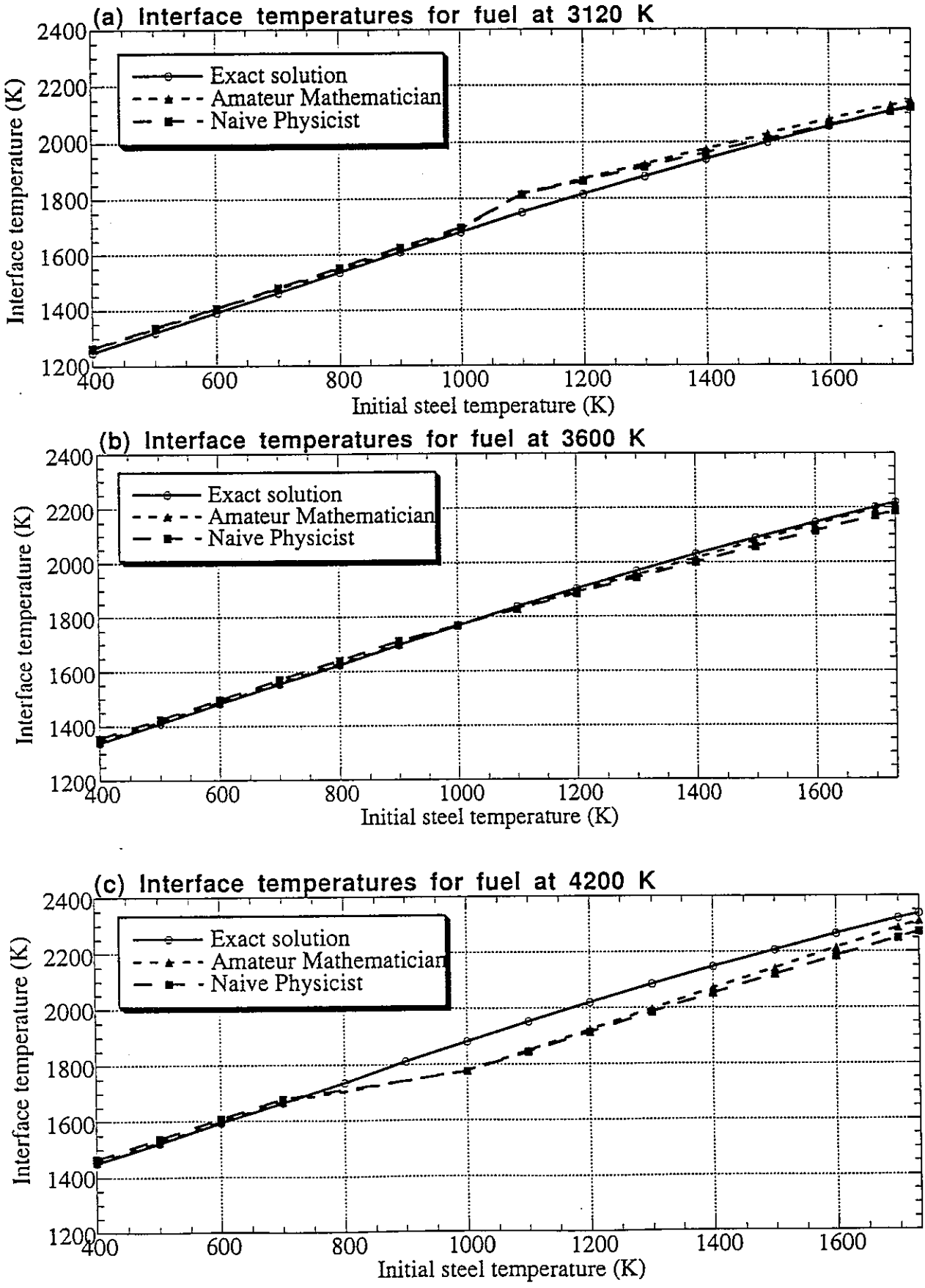

Fig. 14: Fuel-Steel interface temperature using the exact and approximate solutions

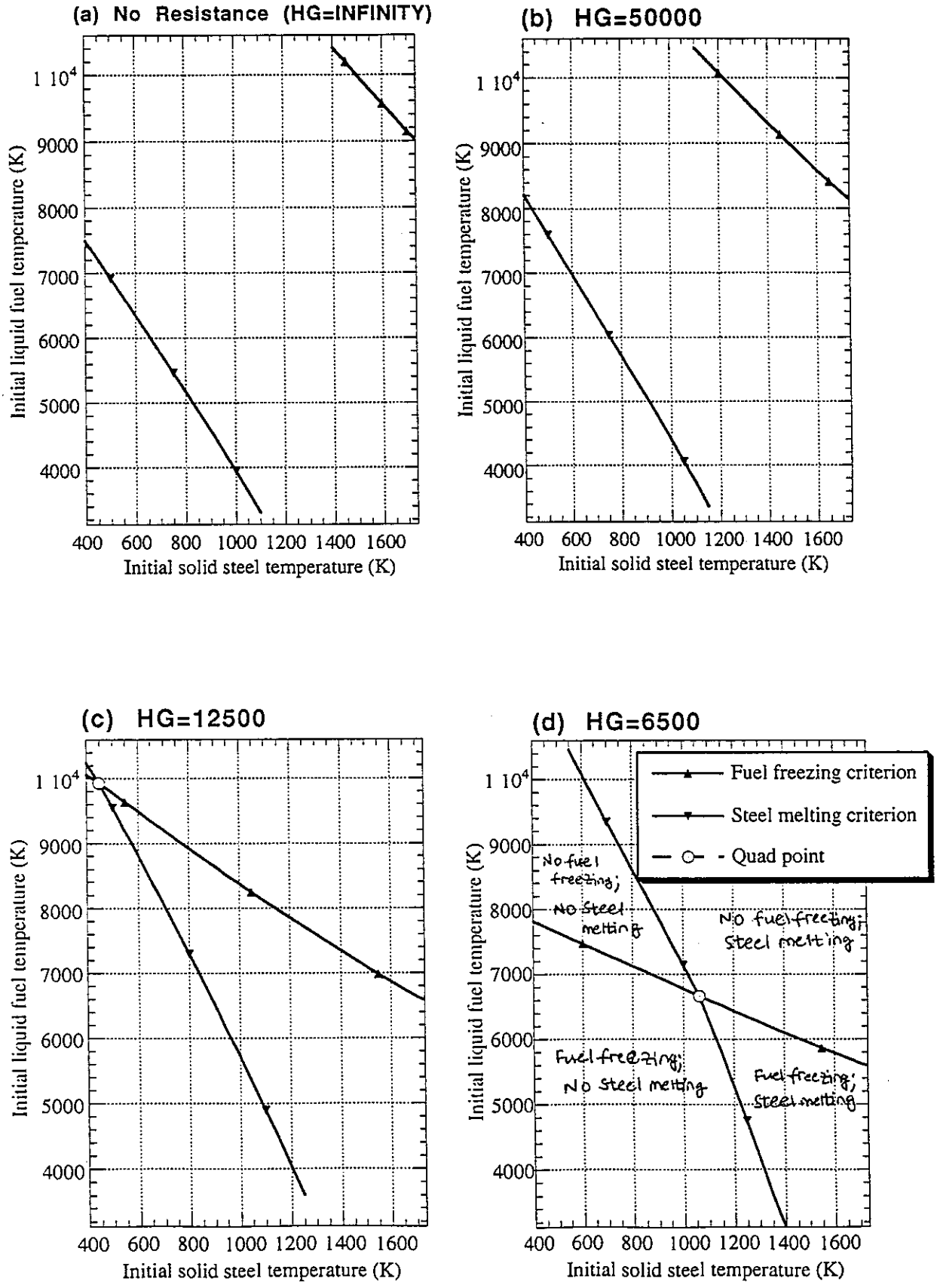

Fig. 15: Effect of an ideal gap conductance on the phase change temperature map (1/2)

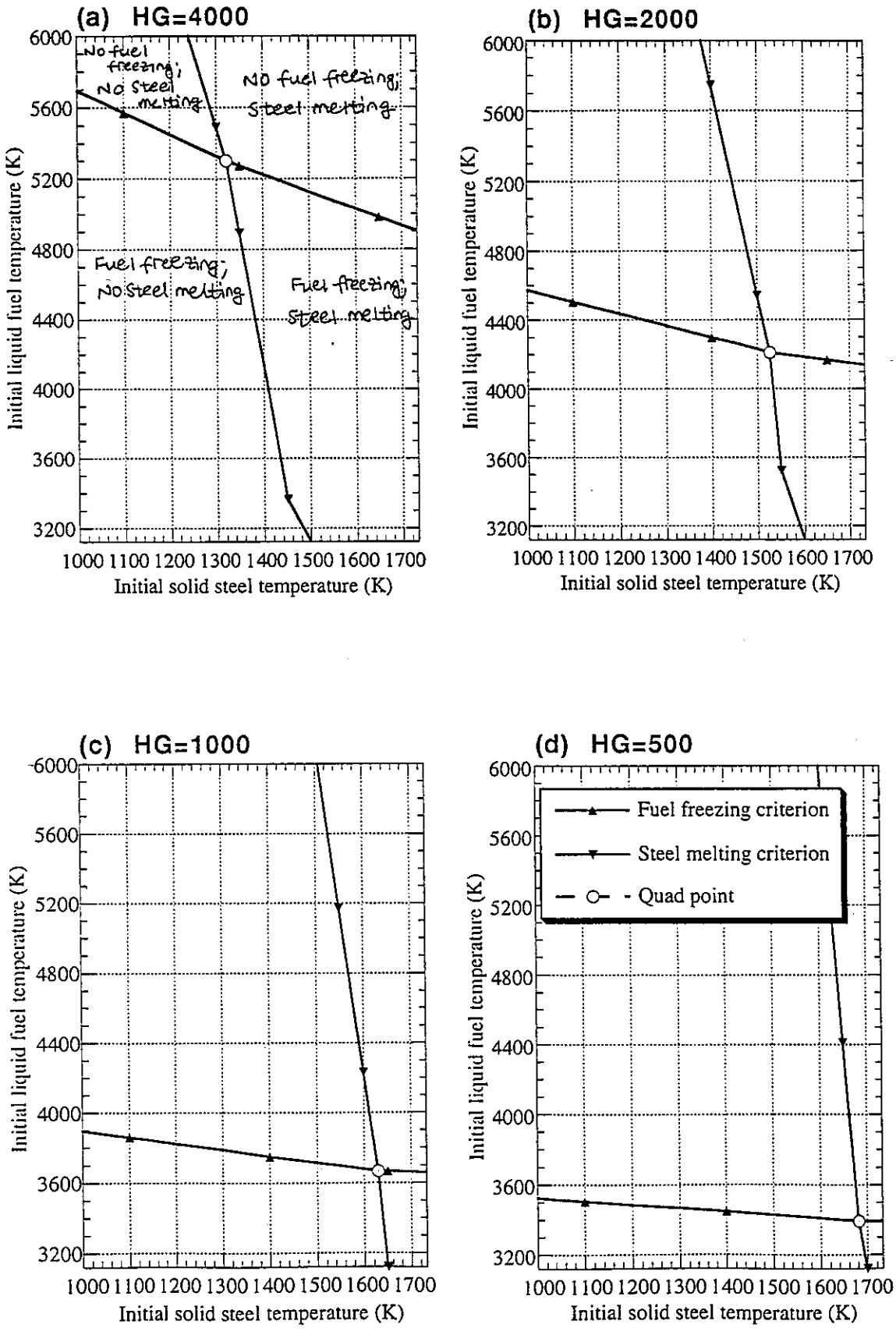

Fig. 16: Effect of an ideal gap conductance on the phase change temperature map (2/2)

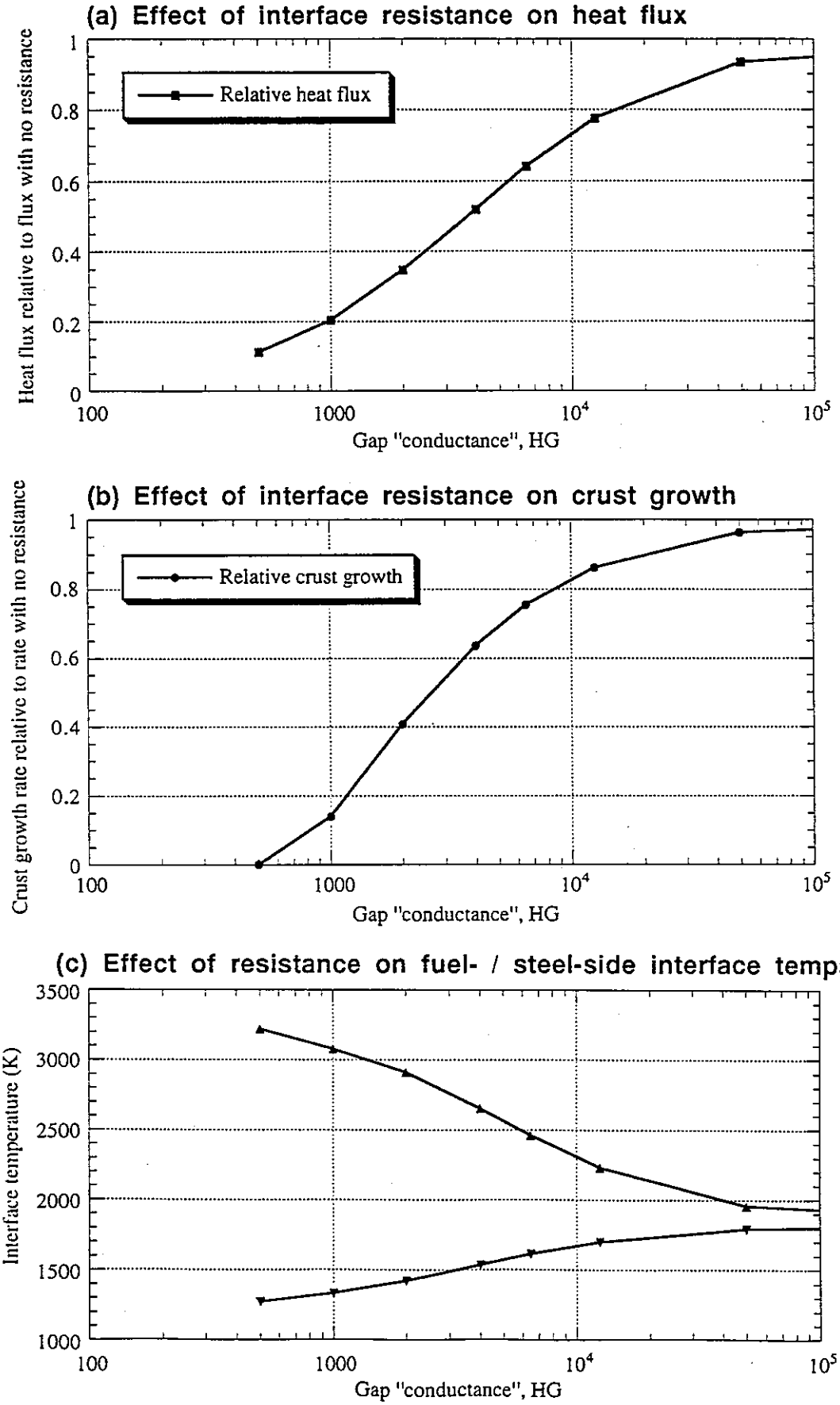

Fig. 17: Effect of an ideal gap conductance on heat flux, crust growth and interface temperatures for fuel initially at 3600 K and structure at 1200 K

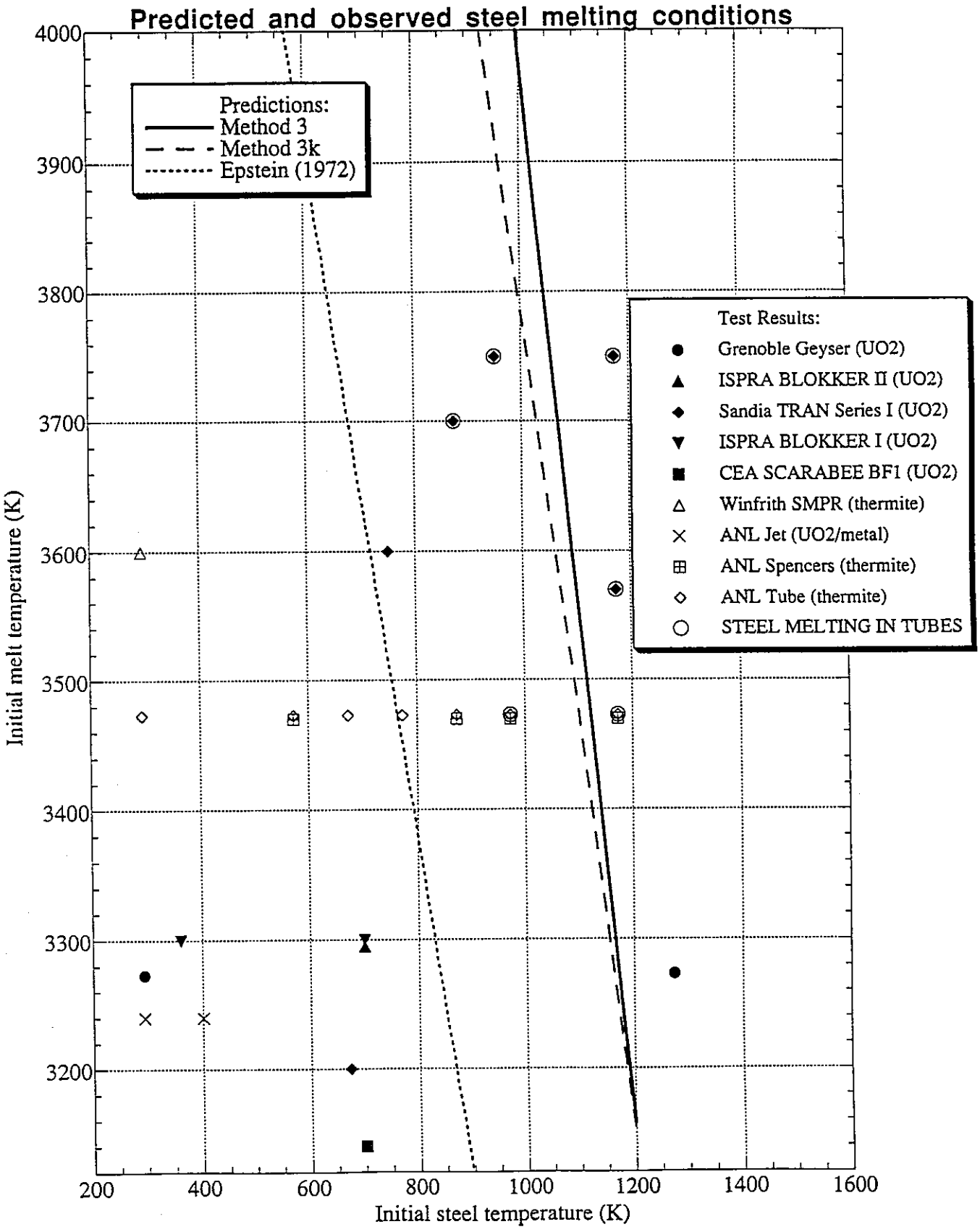

Fig. 18: Predictions of structure melting compared with experimental data

Appendix A

The error function and approximate functions

The error function [A1]

The error function, erf(x), is defined as:

$$\mathrm{erf}(x) = \frac{2}{\sqrt{\pi}} \int_0^x e^{-\xi^2} d\xi \qquad \text{(A-1)}$$

Some properties of the error function which follow from equation (A-1) are:

$$\begin{aligned} &\mathrm{erf}(0) = 0 \\ &\mathrm{erf}(\infty) = 1 \\ &\mathrm{erf}(-x) = -\mathrm{erf}(x) \end{aligned} \qquad \text{(A-2)}$$

The function erfc(x) is defined as:

$$\mathrm{erfc}(x) = 1 - \mathrm{erf}(x) = \frac{2}{\sqrt{\pi}} \int_x^\infty e^{-\xi^2} d\xi \qquad \text{(A-3)}$$

The first derivative of the error function is:

$$\frac{d}{dx}\mathrm{erf}(x) = \frac{2}{\sqrt{\pi}} e^{-x^2} \qquad \text{(A-4)}$$

The error function can also be expressed as a series for small values of x:

$$\mathrm{erf}(x) = \frac{2}{\sqrt{\pi}} \sum_{n=0}^{\infty} \frac{(-1)^n x^{2n+1}}{(2n+1)n!} \qquad \text{(A-5)}$$

Values of the error function are tabulated in Table A.1.

Approximations to the error function

The error function (A-1) is an integral, which is inefficient to calculate by a computer program. Fortunately, good simple approximations to the error function are available [A2].

The error function can be reproduced to at least four significant figures using the following expression:

$$\text{erf}(x) \cong 1 - P(t)e^{-x^2}$$

where $$P(t) = 0.254829592 \times t - 0.284496736 \times t^2 + 1.421413741 \times t^3 - 1.453152027 \times t^4 + 1.061405429 \times t^5 \qquad \text{(A-6)}$$

and $$t = \frac{1}{1 + 0.3275911x}$$

The following formula is a simpler approximation to the error function:

$$\text{erf}(x) \cong \begin{cases} \dfrac{6x}{\pi^{1/2}(3 + x^2)} & \text{for} \quad x \le 1.5 \\ 1 & \text{for} \quad x > 1.5 \end{cases} \qquad \text{(A-7)}$$

The approximating functions (A-6) and (A-7) are compared with values of the error function obtained from tables in Figure A.1.

Approximations to functions involving the error function

The analysis in the main text gives rise to three expressions involving the error function which require a simple, if not crude, approximation. In each case it is required to represent the function by a polynomial not greater than $O(x^2)$.

(a) $$f_1(x) = \frac{e^{-x^2}}{\text{erfc}(x)} \qquad \text{(A-8)}$$

Equation (A-6) suggests that a good approximation to f_1 is:

$$f_1(x) \cong \frac{1}{P(t)} \qquad \text{(A-9)}$$

Equation (A-9) is still too complicated, but has the following properties at its limits:

$$\frac{1}{P(t)} = 1 \quad \text{at} \quad x = 0$$
$$\frac{1}{P(t)} \to \frac{0.3275911}{0.254829592}x \quad \text{as} \quad x \to \infty \qquad \text{(A-10)}$$

The properties in equation (A-10) suggest f_1 can be crudely approximated by a linear function. This assumption is supported by the plot of tabulated values of f_1 in Figure A.2(a). A suitable linear approximation over the range of x of interest is:

$$f_1(x) \approx 1 + 1.35x \qquad \text{(A-11)}$$

$$(b)\quad f_2(x)=\frac{e^{-x^2}}{\mathrm{erf}(x)} \tag{A-12}$$

If the error function is approximated using equation (A-7), and the exponential term is expanded as a series, equation (A-12) becomes:

$$f_2(x)\cong\left(1-x^2+\frac{x^4}{2}-....\right)\frac{\pi^{1/2}}{6}\left(\frac{3}{x}+x\right) \tag{A-13}$$

If we restrict ourselves to terms $O(x^2)$ or less, equation (A-13) becomes:

$$f_2(x)\approx\frac{\pi^{1/2}}{2}\left(\frac{1}{x}-\frac{2}{3}x\right) \tag{A-14}$$

Figure A.2(b) shows that this approximation is valid over the range of x of interest.

$$(c)\quad f_3(x)=\frac{e^{-x^2}}{\mathrm{erf}(x)+x_0} \tag{A-15}$$

Using the same approximations as applied to f_2 , equation (A-15) becomes:

$$f_3(x)\approx\frac{\left(1-2x^2/3\right)}{x_0\left(1+2x/\pi^{1/2}x_0+x^2/3\right)} \tag{A-16}$$

Equation (A-16) is compared with equation (A-15) for three values of x_0 in Figure A.2(c).

References

[A1] Carslaw and Jaeger, "Conduction of heat in solids", Appendix 2, 2nd edition, Oxford University Press (1959).

[A2] Kurz and Fisher, "Fundamentals of solidification", Appendix 1, 3rd edition, Trans Tech Publications Ltd (1992).

Table A.1: Values of the error function

Z	erf(Z)	Z	erf(Z)	Z	erf(Z)	Z	erf(Z)
0.00	0.0000	0.26	0.2869	0.52	0.5379	0.78	0.7300
0.01	0.0113	0.27	0.2974	0.53	0.5465	0.79	0.7361
0.02	0.0226	0.28	0.3079	0.54	0.5549	0.80	0.7421
0.03	0.0338	0.29	0.3183	0.55	0.5633	0.81	0.7480
0.04	0.0451	0.30	0.3286	0.56	0.5716	0.82	0.7538
0.05	0.0564	0.31	0.3389	0.57	0.5798	0.83	0.7595
0.06	0.0676	0.32	0.3491	0.58	0.5879	0.84	0.7651
0.07	0.0789	0.33	0.3593	0.59	0.5959	0.85	0.7707
0.08	0.0901	0.34	0.3694	0.60	0.6039	0.86	0.7761
0.09	0.1013	0.35	0.3794	0.61	0.6117	0.87	0.7814
0.10	0.1125	0.36	0.3893	0.62	0.6194	0.88	0.7867
0.11	0.1236	0.37	0.3992	0.63	0.6270	0.89	0.7918
0.12	0.1348	0.38	0.4090	0.64	0.6346	0.90	0.7969
0.13	0.1459	0.39	0.4187	0.65	0.6420	0.91	0.8019
0.14	0.1569	0.40	0.4284	0.66	0.6494	0.92	0.8068
0.15	0.1680	0.41	0.4380	0.67	0.6566	0.93	0.8116
0.16	0.1790	0.42	0.4475	0.68	0.6638	0.94	0.8163
0.17	0.1900	0.43	0.4569	0.69	0.6708	0.95	0.8209
0.18	0.2009	0.44	0.4662	0.70	0.6778	0.96	0.8254
0.19	0.2118	0.45	0.4755	0.71	0.6847	0.97	0.8299
0.20	0.2227	0.46	0.4847	0.72	0.6914	0.98	0.8342
0.21	0.2335	0.47	0.4937	0.73	0.6981	0.99	0.8385
0.22	0.2443	0.48	0.5027	0.74	0.7047	1.00	0.8427
0.23	0.2550	0.49	0.5117	0.75	0.7112	1.30	0.9340
0.24	0.2657	0.50	0.5205	0.76	0.7175	1.80	0.9891
0.25	0.2763	0.51	0.5292	0.77	0.7238	2.00	0.9953

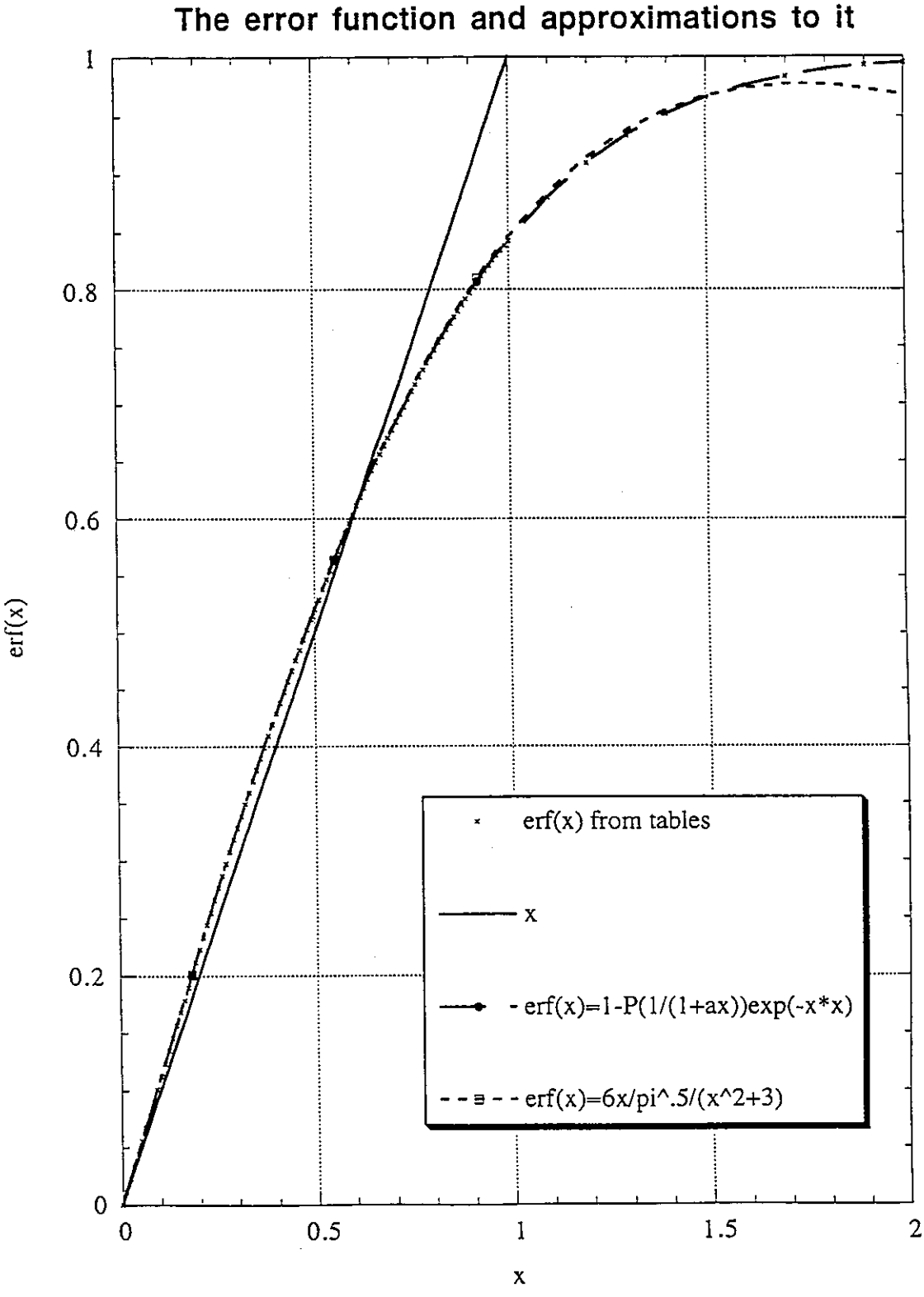

Fig. A.1: The error function and functions which approximate to the error function

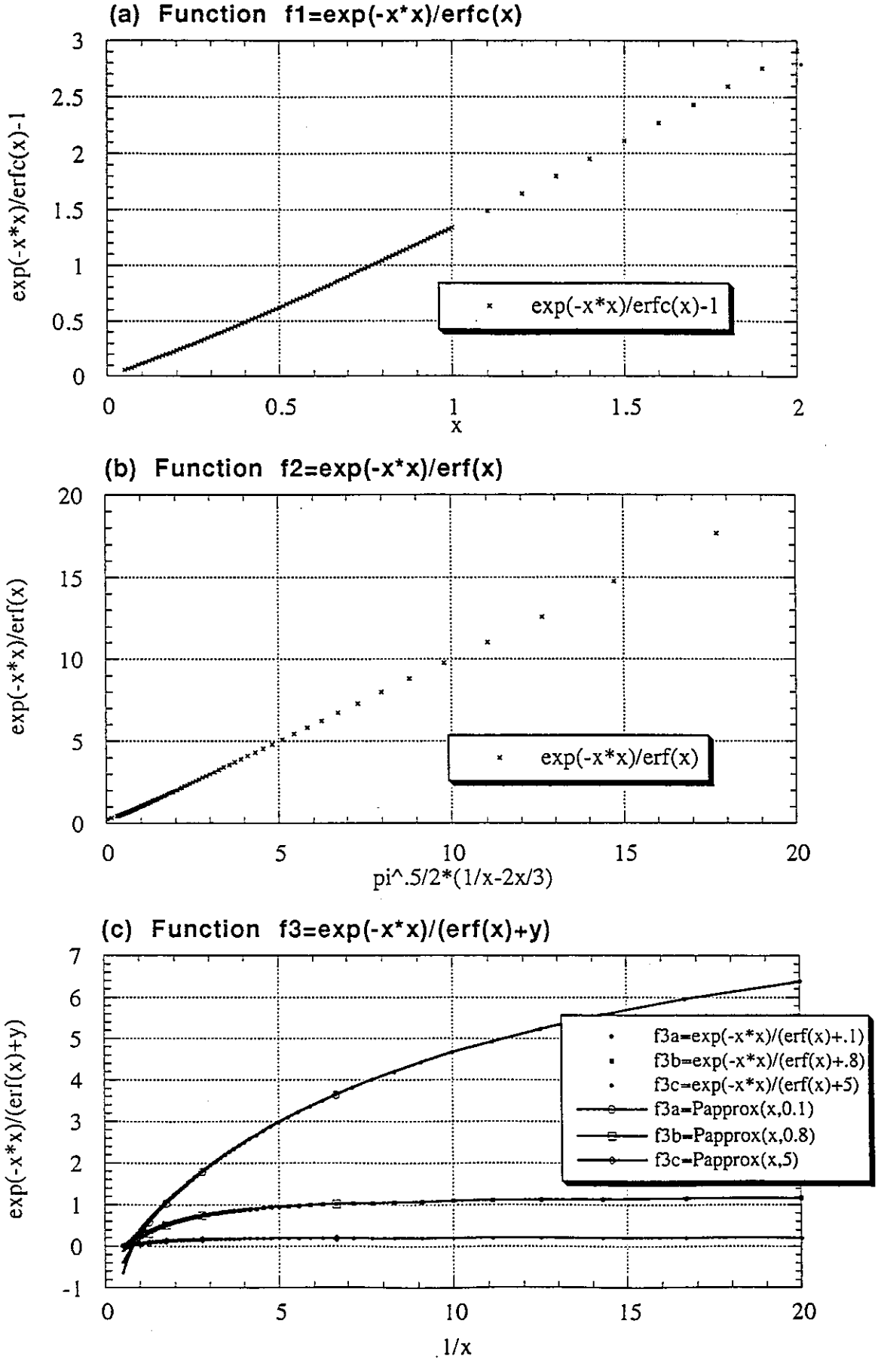

Fig. A.2: Functions which approximate to expressions involving the error function

Appendix B

Materials properties used to perform calculations

All temperatures, T, are in K.

Liquid fuel materials properties functions

Latent heat of fusion, L (J/Kg):

$$L_{fu} = 2.7714 \times 10^5$$

Thermal conductivity, k (W/m/K):

$$k_{fu,l} = 2.5$$

Density, ρ (Kg/m^3):

$$\rho_{fu,l} = 8860. \times \left[\begin{array}{l} 1. - 1.03384 \times 10^{-4} \times (T - 3120) - 1.4803 \times 10^{-10} \times (T - 3120)^2 \\ -3.78342 \times 10^{-16} \times (T - 3120)^3 \end{array} \right] \quad \rho_{fu,l}^{min} = 1560.$$

Specific heat, c (J/Kg/K):

$$c_{fu,l} = 514.01 + 0.0032585 \times T - 8.282 \times 10^{-7} \times T^2 - 2.183 \times 10^{-11} \times T^3$$

$$c_{fu,l}^{min} = 464$$

Solid fuel materials properties functions

Thermal conductivity, k (W/m/K):

$$k_{fu,s} = 4.1629 + \frac{1.0889 \times 10^3}{T} + \frac{4.5853 \times 10^5}{T^2} - 2.5133 \times 10^{-3} \times T + 7.2655 \times 10^{-7} \times T^2$$

Density, ρ (Kg/m^3):

$$\rho_{fu,s} = 10970. \left[1.0056 - 1.6324 \times 10^{-5} \times T - 8.3281 \times 10^{-9} \times T^2 + 2.0176 \times 10^{-13} \times T^3 \right]$$

Specific heat, c (J/Kg/K):

$$c_{fu,s} = 238.955 + 0.105684 T + 2.01177 \times 10^{-6} \times T^2 - 5.15552 \times 10^{-8} \times T^3 + 2.02217 \times 10^{-11} \times T^4 - \frac{2152453}{T^2}$$

$$c_{fu,s}^{max} = 618.6 \qquad \text{for } T > 2670.72 \text{ K}$$

Liquid steel materials properties functions

Latent heat of fusion, L (J/Kg):
$L_{ss} = 3.392 \times 10^5$

Thermal conductivity, k (W/m/K):
$k_{ss,l} = 10.981 + 3.214 \times 10^{-3} \times T$

Density, ρ (Kg/m^3):
$\rho_{ss,l} = 7071.4 - 0.64483 \times (T - 1733)$

Specific heat, c (J/Kg/K):
$c_{ss,s} = 917.37 - 0.099311 \times T + 1.2892 \times 10^{-5} \times T^2$
$c_{ss,l}^{min} = 736$

Solid steel materials properties functions

Thermal conductivity, k (W/m/K):
$k_{ss,s} = 9.735 + 1.434 \times 10^{-2} \times T$

Density, ρ (Kg/m^3):
$\rho_{ss,s} = 7964.6 - 0.25037 \times T - 6.0646 \times 10^{-5} \times T^2 - 6.0868 \times 10^{-9} \times T^3 + 1.9364 \times 10^{-12} \times T^4$

Specific heat, c (J/Kg/K):
$c_{ss,s} = 419.72 + 0.16029 \times T + 3.167 \times 10^{-4} \times T^2 - 2.00 \times 10^{-7} \times T^3$
$c_{ss,s}^{min} = 450$

Notes

All specific heats are at constant pressure.

References

K. Morita, E.A. Fischer and K. Thurnay, "Thermodynamic properties and equations of state for fast reactor safety analysis Part II: Properties of fast reactor materials," Nucl. Eng. Des., in press (1998).

K. Morita, unpublished PNC report, January 1995.

Table B.1: UO_2 and steel properties at their melting points and the temperature arrays used in the Meltit code

```
MATERIAL 1 (FUEL)
-----------------
  Melting temperature (K): TMP1 =    .3120E+04
  Latent heat (J/Kg): HLT1 =    .2771E+06
  Liquid thermal conductivity (W/m/K): CONL1 =    .2500E+01
  Liquid density (Kg/m3): RHOL1 =    .8860E+04
  Liquid specific heat (J/Kg/K): CPL1 =    .5155E+03
  Solid thermal conductivity (W/m/K): CONS1 =    .3790E+01
  Solid density (Kg/m3): RHOS1 =    .9651E+04
  Solid specific heat (J/Kg/K): CPS1 =    .6186E+03

 GROUPINGS:
  ALPHAL1 (m2/s) =    .5474E-06
  ALPHAS1 (m2/s) =    .6349E-06
  ALAM1 =    .5725E+00
  BETA1 =    .1077E+01
  SIGMA1 =    .7104E+00


 MATERIAL 2 (STEEL)
 ------------------
  Melting temperature (K): TMP2 =    .1733E+04
  Latent heat (J/Kg): HLT2 =    .3392E+06
  Liquid thermal conductivity (W/m/K): CONL2 =    .1655E+02
  Liquid density (Kg/m3): RHOL2 =    .7071E+04
  Liquid specific heat (J/Kg/K): CPL2 =    .7840E+03
  Solid thermal conductivity (W/m/K): CONS2 =    .3459E+02
  Solid density (Kg/m3): RHOS2 =    .7334E+04
  Solid specific heat (J/Kg/K): CPS2 =    .6077E+03

 GROUPINGS:
  ALPHAL2 (m2/s) =    .2985E-05
  ALPHAS2 (m2/s) =    .7760E-05
  ALAM2 =    .5529E+00
  BETA2 =    .6203E+00
  SIGMA2 =    .7715E+00


 MORE GROUPINGS
 --------------
  Diff between melting points: DTMP (K) =    .1387E+04
  SIGMAR =    .2014E+01


*** TEMPERATURE ARRAYS

 MATERIAL 1 (FUEL) - No. values: NTFU = 31
 -----------------
  3120. 3200. 3400. 3600. 3800. 4000. 4200. 4400. 4600. 4800.
  5000. 5200. 5400. 5600. 5800. 6000. 6200. 6400. 6600. 6800.
  7000. 7200. 7400. 7600. 7800. 8000. 8200. 8400. 8600. 8800. 9000.

 MATERIAL 2 (STEEL) - No. values: NTSS = 28
 ------------------
   400.  450.  500.  550.  600.  650.  700.  750.  800.  850.
   900.  950. 1000. 1050. 1100. 1150. 1200. 1250. 1300. 1350.
  1400. 1450. 1500. 1550. 1600. 1650. 1700. 1733.
```

Table B.2: Temperature-dependent UO_2 properties

SOLID FUEL PROPERTIES

Fuel temp. (K)	Conductivity W/m/k	Density Kg/m3	Heat Capacity J/Kg/K	Diffusivity m2/s
Epstein:	2.1	-	504	.42e-6
1733.0	.2770E+01	.1046E+05	.3415E+03	.7757E-06
1871.7	.2717E+01	.1039E+05	.3533E+03	.7400E-06
2010.4	.2702E+01	.1032E+05	.3704E+03	.7067E-06
2149.1	.2723E+01	.1025E+05	.3945E+03	.6736E-06
2287.8	.2779E+01	.1017E+05	.4275E+03	.6393E-06
2426.5	.2869E+01	.1009E+05	.4713E+03	.6032E-06
2565.2	.2991E+01	.1001E+05	.5283E+03	.5656E-06
2703.9	.3144E+01	.9923E+04	.6186E+03	.5123E-06
2842.6	.3329E+01	.9835E+04	.6186E+03	.5472E-06
2981.3	.3545E+01	.9744E+04	.6186E+03	.5880E-06
3120.0	.3790E+01	.9651E+04	.6186E+03	.6349E-06

LIQUID FUEL PROPERTIES

Fuel temp. (K)	Conductivity W/m/k	Density Kg/m3	Heat Capacity J/Kg/K	Diffusivity m2/s
Epstein:	2.1	-	-	.42e-6
3120.0	.2500E+01	.8860E+04	.5155E+03	.5474E-06
3200.0	.2500E+01	.8787E+04	.5152E+03	.5522E-06
3400.0	.2500E+01	.8603E+04	.5147E+03	.5646E-06
3600.0	.2500E+01	.8420E+04	.5140E+03	.5777E-06
3800.0	.2500E+01	.8237E+04	.5132E+03	.5914E-06
4000.0	.2500E+01	.8053E+04	.5124E+03	.6059E-06
4200.0	.2500E+01	.7869E+04	.5115E+03	.6211E-06
4400.0	.2500E+01	.7685E+04	.5105E+03	.6373E-06
4600.0	.2500E+01	.7501E+04	.5093E+03	.6543E-06
4800.0	.2500E+01	.7317E+04	.5082E+03	.6723E-06
5000.0	.2500E+01	.7133E+04	.5069E+03	.6914E-06
5200.0	.2500E+01	.6949E+04	.5055E+03	.7117E-06
5400.0	.2500E+01	.6765E+04	.5040E+03	.7332E-06
5600.0	.2500E+01	.6580E+04	.5025E+03	.7561E-06
5800.0	.2500E+01	.6396E+04	.5008E+03	.7805E-06
6000.0	.2500E+01	.6211E+04	.4990E+03	.8066E-06
6200.0	.2500E+01	.6026E+04	.4972E+03	.8344E-06
6400.0	.2500E+01	.5841E+04	.4952E+03	.8642E-06
6600.0	.2500E+01	.5656E+04	.4932E+03	.8962E-06
6800.0	.2500E+01	.5471E+04	.4910E+03	.9306E-06
7000.0	.2500E+01	.5286E+04	.4888E+03	.9677E-06
7200.0	.2500E+01	.5101E+04	.4864E+03	.1008E-05
7400.0	.2500E+01	.4915E+04	.4839E+03	.1051E-05
7600.0	.2500E+01	.4730E+04	.4814E+03	.1098E-05
7800.0	.2500E+01	.4544E+04	.4787E+03	.1149E-05
8000.0	.2500E+01	.4358E+04	.4759E+03	.1205E-05
8200.0	.2500E+01	.4173E+04	.4730E+03	.1267E-05
8400.0	.2500E+01	.3987E+04	.4700E+03	.1334E-05
8600.0	.2500E+01	.3800E+04	.4669E+03	.1409E-05
8800.0	.2500E+01	.3614E+04	.4640E+03	.1491E-05
9000.0	.2500E+01	.3428E+04	.4640E+03	.1572E-05

Table B.3: Temperature-dependent steel properties

SOLID STEEL PROPERTIES

Steel temp. (K)	Conductivity W/m/k	Density Kg/m3	Heat Capacity J/Kg/K	Diffusivity m2/s
Epstein:	16	-	-	.444e-5
400.0	.1547E+02	.7854E+04	.5217E+03	.3776E-05
450.0	.1619E+02	.7839E+04	.5378E+03	.3840E-05
500.0	.1690E+02	.7824E+04	.5540E+03	.3900E-05
550.0	.1762E+02	.7808E+04	.5704E+03	.3957E-05
600.0	.1834E+02	.7791E+04	.5867E+03	.4012E-05
650.0	.1906E+02	.7775E+04	.6028E+03	.4066E-05
700.0	.1977E+02	.7758E+04	.6185E+03	.4121E-05
750.0	.2049E+02	.7741E+04	.6337E+03	.4177E-05
800.0	.2121E+02	.7723E+04	.6482E+03	.4236E-05
850.0	.2192E+02	.7705E+04	.6620E+03	.4298E-05
900.0	.2264E+02	.7687E+04	.6747E+03	.4365E-05
950.0	.2336E+02	.7668E+04	.6863E+03	.4438E-05
1000.0	.2407E+02	.7649E+04	.6967E+03	.4517E-05
1050.0	.2479E+02	.7630E+04	.7057E+03	.4604E-05
1100.0	.2551E+02	.7611E+04	.7130E+03	.4701E-05
1150.0	.2623E+02	.7591E+04	.7187E+03	.4807E-05
1200.0	.2694E+02	.7570E+04	.7225E+03	.4926E-05
1250.0	.2766E+02	.7550E+04	.7243E+03	.5058E-05
1300.0	.2838E+02	.7529E+04	.7239E+03	.5207E-05
1350.0	.2909E+02	.7508E+04	.7212E+03	.5373E-05
1400.0	.2981E+02	.7486E+04	.7161E+03	.5561E-05
1450.0	.3053E+02	.7464E+04	.7083E+03	.5775E-05
1500.0	.3124E+02	.7442E+04	.6977E+03	.6017E-05
1550.0	.3196E+02	.7419E+04	.6843E+03	.6296E-05
1600.0	.3268E+02	.7397E+04	.6677E+03	.6617E-05
1650.0	.3340E+02	.7373E+04	.6480E+03	.6990E-05
1700.0	.3411E+02	.7350E+04	.6249E+03	.7427E-05
1733.0	.3459E+02	.7334E+04	.6077E+03	.7760E-05

LIQUID STEEL PROPERTIES

Steel temp. (K)	Conductivity W/m/k	Density Kg/m3	Heat Capacity J/Kg/K	Diffusivity m2/s
Epstein:	16	-	-	.444e-5
1733.0	.1655E+02	.7071E+04	.7840E+03	.2985E-05
1871.7	.1700E+02	.6982E+04	.7767E+03	.3134E-05
2010.4	.1744E+02	.6893E+04	.7698E+03	.3287E-05
2149.1	.1789E+02	.6803E+04	.7635E+03	.3444E-05
2287.8	.1833E+02	.6714E+04	.7576E+03	.3604E-05
2426.5	.1878E+02	.6624E+04	.7523E+03	.3768E-05
2565.2	.1923E+02	.6535E+04	.7475E+03	.3936E-05
2703.9	.1967E+02	.6445E+04	.7431E+03	.4107E-05
2842.6	.2012E+02	.6356E+04	.7392E+03	.4282E-05
2981.3	.2056E+02	.6266E+04	.7360E+03	.4458E-05
3120.0	.2101E+02	.6177E+04	.7360E+03	.4621E-05

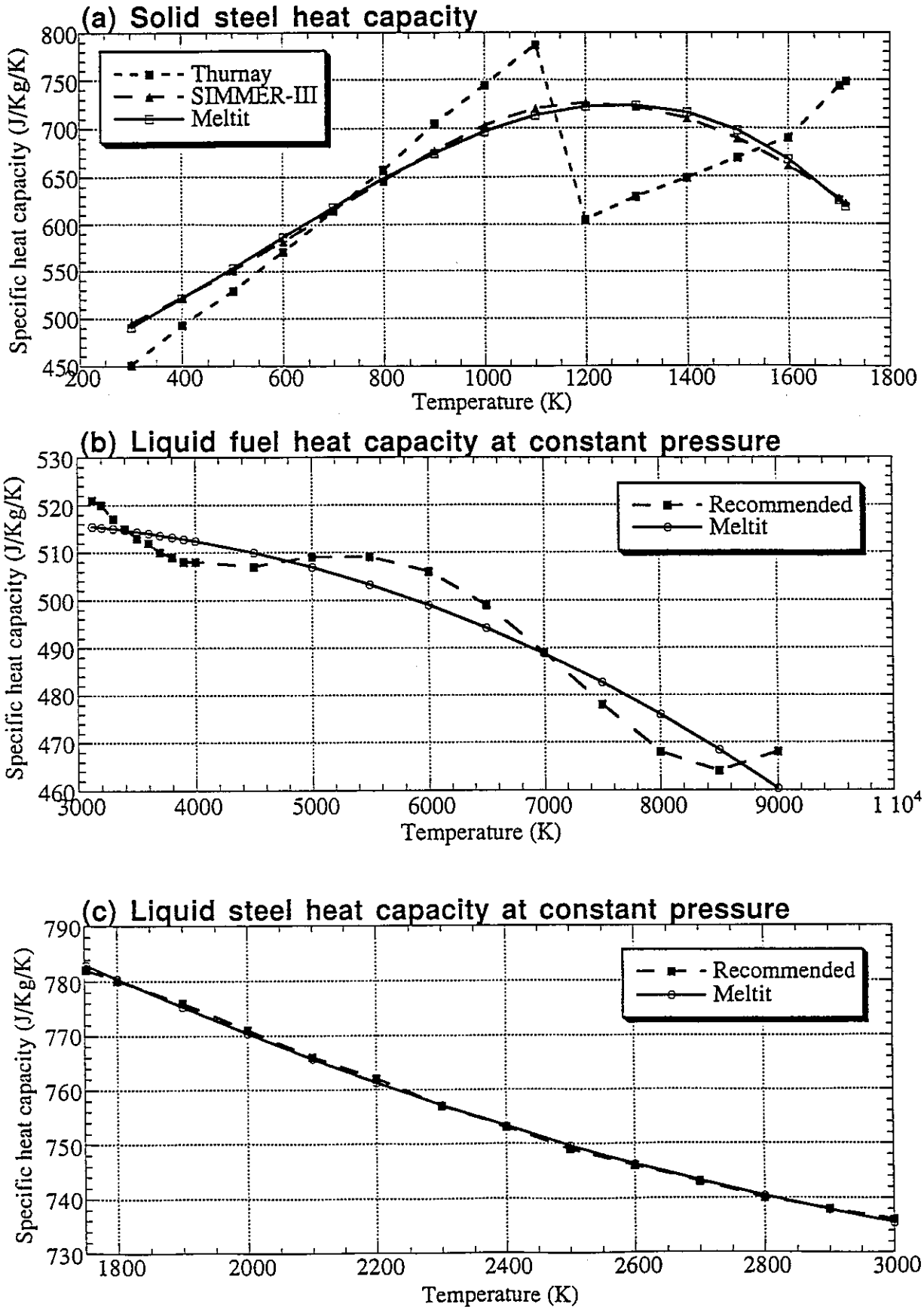

Fig. B.1: The functions used to calculate heat capacities of UO_2 and steel in Meltit